NASA
Technical Memorandum 4334

AVSCOM
Technical Report 92-B-004

Experimental Evaluation of a Flat Wake Theory for Predicting Rotor Inflow-Wake Velocities

John C. Wilson

APRIL 1992

NASA
Technical Memorandum 4334

AVSCOM
Technical Report 92-B-004

Experimental Evaluation of a Flat Wake Theory for Predicting Rotor Inflow-Wake Velocities

John C. Wilson
Aeroflightdynamics Directorate—AVSCOM
JRPO—Langley
Langley Research Center
Hampton, Virginia

National Aeronautics and
Space Administration

Office of Management

Scientific and Technical
Information Program

1992

Summary

The theory for predicting helicopter inflow-wake velocities called *flat wake theory* was correlated with several sets of experimental data. The theory was developed by V. E. Baskin of the USSR in 1976, and a computer code known as DOWN was developed later at Princeton University to implement the theory. The theory treats the wake geometry as rigid without interaction between induced velocities and wake structure. The wake structure is assumed to be a flat sheet of vorticity composed of trailing elements whose strength depends on the azimuthal and radial distribution of circulation on a rotor blade. The code predicts the three orthogonal components of flow velocity in the field surrounding the rotor. The predictions can be utilized in rotor performance and helicopter real-time flight-path simulation. The predictive capability of the coded version of the theory was correlated with flow velocity data from several sources. In general, the coded version of flat wake theory provides vertical inflow patterns similar to experimental patterns. Several descriptions of rotor blade circulation were used in the code to bring about a better fit of prediction of vertical inflow to measurement, but none were wholly satisfactory. To some extent, the disparities may be attributed to rotor-hub wake effects. However, the fundamental wake modeling of flat wake theory may not be adequate for improving the correlation of code prediction with experimental data. Several assumptions are made in the theory that may contribute to the disparity between prediction and data.

Introduction

The prediction of inflow to a helicopter rotor and the wake-induced velocities are vital to the calculation of airloads on the rotor blades of a helicopter and on the other components. Inflow and wake velocities affect the local angles of attack and, therefore, the airloads that the helicopter rotor and other components experience. Many theories and analyses have been developed for such predictions of both mean and time-varying inflow-wake patterns. Some of these are described in references 1–17. Computer codes to implement these predictions have grown in complexity as the theories have grown in complexity. Rotor performance codes use inflow models that range from the assumption of uniform inflow to complex, time-varying, vortex filament, "free-wake" models that compute complex inflow distributions at the rotor disk. These generally ignore the effects of the fuselage on the velocities seen by elements of the lifting rotor. Even though computer processing time and associated costs have dramatically decreased in recent years, there is still a need for codes that are simple and fast *and*, at the same time, offer accurate representations of inflow and wake patterns (as mentioned in refs. 12, 17, and 18).

"Real-time" simulation of helicopter flight for agility and controllability studies requires faster and more representative inflow-wake modeling (ref. 17). Reference 18 concludes that an understanding of the influence of the rotor wake on the fixed tail surfaces and tail rotor is one of the most important factors needed to improve the representation of helicopter flight path motions. Reference 19, which describes the development history of the U.S. Army's AH-64 helicopter, provides examples of the importance of the wake interaction between the main rotor, tail rotor, and empennage. The empennage design had to be changed as a better understanding of wake effects evolved.

The calculation of dynamic rotor characteristics has depended generally on the assumption of uniform inflow (invariant with azimuth or radial position). This, of course, is unrealistic. As early as 1934, Wheatley concluded in reference 1 that "The blade motion is critically dependent upon the distribution of induced velocities over the rotor disk and cannot be calculated rigorously without the accurate determination of the induced flow." In recent years more sophisticated (and complex) inflow descriptions have come into use, but as noted in reference 17, these have not generally resulted in significantly better predictions.

A theory that may offer an acceptable balance of speed and prediction capability for mean inflow-wake velocity has been used in Eastern Europe and is referred to as the *flat wake theory* (ref. 20). The theory and associated assumptions and limitations are well-described in references 20, 21, and 22. The theory involves assuming a rigid undeflected ribbon of vorticity generated by the rotor blades as shown in figure 1. The vortices transferred from the rotor blades to the slipstream of the rotor are assumed to merge to a single ribbon of vorticity trailing behind the rotor. At advance ratios greater than 0.13 (52 knots for a typical rotor system), the nonlinearities of the vortex motion are judged in reference 20 to have a minor influence on the induced velocities near the rotor disk plane. The flat wake theory is most useful for predicting time-averaged inflow and wake characteristics about a rotor. Since the prediction is only from a time-averaged sense, it is assumed to be unaffected by blade passage. For a time-varying rotor flow field analysis, references 11–15 can provide an estimate of the influence of blade passage.

Such theories are useful for time-varying blade loads, rotor dynamics analyses, and rotor acoustics.

The results in reference 20 indicate good agreement with some experimental measurements of the velocity components in the wake of a lifting rotor. The details of the calculation procedure developed for reference 20 were unavailable, and the data used for validation were limited to wake velocity measurements (not inflow); therefore, a study of the flat wake theory and its possible application as a computer code with an acceptable balance of speed and prediction capability was initiated. Using the guidelines offered in references 20 and 21, a relatively compact computer code known as DOWN for the implementation of the flat wake theory was developed in recent years by Howard C. Curtiss and Robert M. McKillup of Princeton University with a NASA research grant. A user's guide (ref. 23) is available for the code.

Predictions of inflow and wake velocities from DOWN are compared with the data of several sources. Until recent years there has been very limited experimental data describing rotor inflow and wake (mostly in ref. 5). This deficiency has been partially remedied with the data presented in references 24–34. These data consist of measurements of the longitudinal and vertical velocity increments caused by a rotor for a variety of advance ratios, rotor blade planforms, and measurement planes. The data of references 24–34 have been used for the evaluation of other inflow-wake analyses (refs. 11, 35, and 36). Some of these data, along with what is available describing rotor flow field characteristics in reference 5, offer a means for the calibration of DOWN. The vertical induced velocity component is of greatest interest since it is critical in the calculation procedures for rotor performance analyses. The lateral component of induced velocity affects sidewash flow angles in the region of a helicopter vertical fin and tail rotor, thus affecting helicopter yaw stability and control. The limited available data in reference 37 describing lateral velocities are also used in the calibration of DOWN.

Symbols

The coordinate system is shown in figure 2. Note that this convention differs from the one used in the United States.

C_T	rotor thrust coefficient, $T/[\rho_a(\Omega R)^2\pi R^2]$
G1, G2, G3	assumed circulation distribution on rotor blade without azimuthal variation (correction), $\Gamma'(\rho)$
G1m, G2m, G3m	assumed circulation distribution on rotor blade with azimuthal variation (correction), $\Gamma'(\rho) + \Gamma'(\mu, \psi)$
R	rotor radius, ft
r	rotor blade station, ft
Δr	increment in rotor blade station, ft
T	rotor thrust, lb
V	flight speed, ft/sec or knots
V_t	rotor tip speed, ΩR, ft/sec
v_x	increment in longitudinal velocity (positive forward) due to rotor inflow and wake, ft/sec
v_y	increment in vertical velocity (positive up) due to rotor inflow and wake, ft/sec
v_z	increment in sidewash velocity (positive right) due to rotor inflow and wake, ft/sec
x, y, z	Cartesian coordinate system centered in rotor hub with x positive forward, y positive upward, and z positive laterally to right (convention used in ref. 20 whereby xz is the tip path plane); nondimensionalized by radius, R (see fig. 2)
α	angle of attack of rotor, deg
Γ	relative circulation averaged around rotor, ft^2/sec
Γ'	blade circulation, ft^2/sec
$\Delta\Gamma$	increment in blade circulation as a function of azimuth, ft^2/sec
$\Delta\eta$	increment in sidewash velocity ratio, v_z/V_t
$\Delta\lambda$	increment in rotor inflow ratio, v_y/V_t
μ	advance ratio, V/V_t
ρ	rotor blade station, r/R
$\Delta\rho$	increment in rotor radius, $\Delta r/R$

ρ_a	air density, slugs/ft^3
ψ	blade azimuth position, deg
Ω	rotor rotational speed, radians/sec

Discussion of Theory and Computer Code

Theory

The development of the flat wake theory and an outline of the means to implement it are described in references 20 and 21. It begins with the consideration of an idealized rotor vortex system that is formed by shed and trailing vortices formed by a rotor blade in hover or axial flight. These form a sheet of vorticity of a classical helical shape called *the vortex sheet* behind each blade (fig. 3). In axial flight, i.e., hover or vertical climb, the sheets of several rotor blades appear to form a column. The column has an axis that is perpendicular to the rotor disk. In horizontal flight an inplane component of velocity results and the axis of the column is skewed with respect to the rotor. As the horizontal flight velocity component increases, the column of vorticity below the rotor deflects more to the rear. At sufficiently high flight speeds, the column becomes practically flat and results in a "ribbon" of vorticity transported downstream at the free-stream velocity (fig. 1). Within this ribbon the trailing vortices leaving the blade have a cycloidal form (fig. 4(a)). These trailing vortex elements are chosen to start at several locations along the blade span and result in a trajectory that suggests a weaving of the vortices within the ribbon. The ribbon is assumed to be a "rigid" wake, and therefore there is no deformation of the wake structure because of wake induced velocities.

The trailing vortices that are formed are the consequence of radial and azimuthal distributions of circulation on the rotor blade. The variation of circulation along the blade span leads to the presence of trailing vortices springing from the blade. As a first approximation, Baskin (ref. 20) assumes that the variation of circulation with azimuth may be neglected for practical calculations if, at each blade station, the circulation is averaged over a complete rotor revolution where in

$$\Gamma(\rho, \mu, \psi) \approx \Gamma'(\rho) + \Delta\Gamma(\mu, \psi)$$

we have

$$\Delta\Gamma(\mu, \psi) = 0$$

However, he does offer a generalization to this first approximation to account for azimuthal variation. Neglecting higher order terms, this becomes

$$\Delta\Gamma(\mu, \psi) \approx -1.5\mu \sin\psi + 1.12\mu^2(1 - \cos 2\psi)$$

He also assumes that the bound vorticity contribution to velocity increments can be ignored. He states that bound vortices having the same circulation at all azimuth angles would not generate any vertical induced velocities. However, they would produce rotational induced velocities at points located above as well as below the rotor disk. On the average, the rotational induced (inplane) velocity represents no more than 0.5 percent of the blade tip speed and can be neglected.

Although this classical helical wake representation has been shown to be a good representation of the physical characteristics of the rotor wake, mathematical implementation of this geometry can be quite extensive and too complex for predesign and real-time simulation analytical methods. Therefore, Baskin has developed an equivalent rectilinear wake structure involving lateral and longitudinal vortices. (See fig. 4.) The rotor system is represented as a lifting disk with a lattice of vortices distributed in a rectilinear fashion. Radial and azimuthal variations in rotor circulation over the disk and their effect in the shed wake can be accounted for at each of the "nodes" of the lattice. The wake is represented by a system of longitudinal trailing vortices from each of the lateral lattice locations (fig. 4(b)). No transverse or shed vorticity is modeled in the wake.

In computing the resultant induced velocity, the velocity components generated by various vortex subsystems forming the wake can be computed separately and then superimposed. The Biot-Savart law is used in the calculation of the field-point velocities induced from each of the lateral and longitudinal vortex segments. Reference 21 offers a detailed description of the contributions of the various vortices to the v_x, v_y, and v_z components and of the process of summation.

Experience and theoretical considerations cited in reference 20 indicate that this flat wake of vorticity is applicable for an advance ratio μ greater than $1.63\sqrt{C_T}$. For a typical rotor tip speed of 700 ft/sec and $C_T = 0.006$, the corresponding advance ratio is approximately 0.13 and the flight speed is 52 knots. In reference 16 Ormiston agrees that "A simple, flat planar wake has been found to be a valid configuration for the wake vorticity down to advance ratios of approximately 0.15 for a nominal rotor thrust coefficient." If a sinusoidal variation of rotor blade circulation with azimuth angle is allowed (as suggested

by refs. 6, 16, and 20), the flat wake analysis may be applicable at a moderately lower advance ratio.

Computer Code

The study and computer coding of flat wake theory of reference 20 was arranged with a NASA research grant to Princeton University. The computer code known as DOWN that evolved can be used to calculate mean induced flow field velocities (vertical, longitudinal, and lateral) with few input parameters (μ, C_T, and location of prediction plane) for rotor operating conditions. A selected circulation distribution on the rotor blade as a function of radius must be defined that is to represent an average for 1 revolution. These are identified in the figures by G1, G2, or G3. Here, G1 represents a linear distribution, G2 represents a modified "parabolic" distribution, and G3 represents a modified "quartic" distribution. The respective equations are as follows:

For G1,

$$\Gamma' = 10.0(0.0589 + 1.3783\rho)$$

for G2,

$$\Gamma' = 10.0(\rho^2 - \rho^3)$$

and for G3,

$$\Gamma' = [(1.0 - 0.685\rho)\rho(\rho^2 + 0.011)]/(\rho^2 + 0.0055)$$

Figure 5 shows these circulation distributions as a function of blade radius where the patterns are carried into the hub and the blade root cutout is ignored. The quartic distribution is more representative of those shown in reference 38 than of either the linear or parabolic distributions. The user of the program DOWN can easily introduce alternate distributions and also has the option of implementing the azimuthal correction suggested by Baskin in reference 20. When the azimuthal correction is used in this paper, the circulation distributions are identified as G1m, G2m, and G3m.

The circulation distribution on a rotor blade is normalized within the code as follows:

$$\Gamma'_{\text{normal}} \equiv \frac{\Gamma'(\rho)}{2\int_0^1 \Gamma'(\rho)\rho\, d\rho}$$

so that any distribution may be used. There is then a summation of incremental velocity components (in the Cartesian coordinate system) that are a function of the incremental change of circulation distribution spanwise (in the polar coordinate system) on the rotor blade. Within the code the increment in radius can be changed. Generally, a selection of increment in radius $\Delta\rho$ of 0.1 and the associated increment (or decrement) in circulation strength are adequate. Using smaller increments does improve accuracy, but experience cited in reference 20 indicates that the gain is not significant. Both the "reversed flow region" and the local blade stalled angle of attack due to interaction with blade tip vortices are not accounted for; also the influence of the wake of the rotor hub is not accounted for. However, these effects are typically ignored in other simple inflow analyses as well in more complex methods (ref. 17).

The code provides tabulations of induced velocity components normalized with tip speed in either Cartesian or cylindrical coordinate systems with two dependent coordinates. The axes convention of reference 20 is maintained (fig. 2) even though it differs from the U.S. convention.

Experimental Data

The data that are used for the calibration of the flat wake code are described in the order used for correlation, and the test conditions are listed in table I.

Experimental Data From Reference 20

The data presented in reference 20 are mean wake velocity measurements for an advance ratio of 0.15 and a thrust coefficient of 0.006. There is no other information regarding rotor angle of attack, power, propulsive force, or data accuracy. The test apparatus and flow measurement technique used are not described. The rotor appears to have had tapered planform blades. The data, which are mean vertical wake velocities nondimensionalized with rotor tip speed, are rather limited for an evaluation of the original version of the flat wake analysis. Baskin was able to obtain a good fit of flat-wake-theory prediction to these data, as shown in figure 6.

Experimental Data From References 24–34

The data presented in references 24–34 are laser velocimetry measurements of longitudinal and vertical velocities one blade chord or less above the rotor tip path plane. Test conditions of advance ratio, thrust coefficient, rotor angle of attack, and measurement plane height are listed in table I. Other rotor operating conditions such as power, propulsive force, etc., can be found in the references. Velocity measurement accuracy was defined in references 24–34 as approximately 2 percent, which translates into an accuracy for $\Delta\lambda$ ranging from approximately ± 0.0002 at $\mu = 0.149$ to ± 0.0008 at $\mu = 0.400$. The measurement locations were made at radial stations from

$\rho = 0.2$ to $\rho = 1.2$ at every 30° of azimuth. The measurements are nondimensionalized with rotor tip speed V_t for both mean and time-varying velocities. For the purpose of evaluating the flat wake code, only the mean data from references 24, 25, 26, 29, and 30 were utilized for this report. These provide the data obtained in a plane parallel to and 1 chord above the rotor tip path plane for rectangular planform blades operated at advance ratios of 0.15, 0.23, 0.30, 0.35, and 0.40, respectively.

These data were obtained with a two-component laser velocimeter (LV) system operated in the NASA Langley 14- by 22-Foot Subsonic Tunnel (ref. 39). The LV system measured the instantaneous components of velocity in the longitudinal and vertical directions. A general-purpose rotorcraft model system called the 2-meter rotor test system (2MRTS) was part of the experimental apparatus. A more detailed description of the 2MRTS is provided in reference 40. The rotor model provided a reasonable representation of rotor, hub, and fuselage so that the hub and the presence of the fuselage affect flow velocities in a manner similar to that on full-scale helicopters.

Experimental Data From Reference 5

In reference 5, Heyson and Katzoff described a theoretical and experimental investigation of the velocities near a lifting rotor. The analysis and data have been used for many years for helicopter design. Mean flow velocity measurements were made above and below the rotor using five-hole pressure-measuring probes. Velocity measurement accuracy was 4 percent with a corresponding accuracy of $\Delta\lambda$ of ± 0.0015 for the data used herein. The model had a teetering rotor system with two untapered, untwisted blades with NACA 0012 airfoils. The rotor test apparatus had no fuselage where the rotor was driven by a shaft enclosed within a tall cylindrical windshield. Thrust coefficients ranged from 0.00321 to 0.00373, tip speed ranged from 450 to 500 ft/sec, and disk loading ranged from 1.55 to 2.21 lb/sq ft. Data were obtained for advance ratios of 0.095, 0.139, 0.140, and 0.232.

Thrust coefficients, tip speed, and disk loading were quite low compared with typical conditions for current helicopters. Both test and analysis of reference 5 deal with lightly loaded rotors and, as pointed out in reference 3, may pose serious limitations to the results. As a cylinder, the windshield may have had a greater effect on flow velocities than would be the case for a fuselage representation as in references 24–34. It is acknowledged in reference 5 that the windshield affected the flow patterns. Although most data and analysis of reference 5 were for rotor and test conditions that are not representative of current rotors and flight conditions, the information for $\mu = 0.232$ is useful for the calibration of the flat-wake-theory code.

Experimental Data From Reference 37

The primary purpose of the wind tunnel program described in reference 37 was to gain an understanding of the flow field environment just ahead of the empennage system as affected by the hub and rotor wake. The fuselage was a model of a U.S. Army attack helicopter. Wake surveys were made that defined the downwash and sidewash angles and the dynamic pressure ratios in that region. The surveys were made at four vertical heights, but since the rotor used in the test was undersized, the effective longitudinal location was $x = -1.76$. (A typical helicopter vertical tail position would be $x \approx -1.20$.) The model fuselage was 30 percent scale, whereas the rotor was 21 percent scale. Wake measurements were obtained both with and without rotor blades so that hub wake effects could be defined. Since the hub was not removed, a definitive appraisal of purely hub effects could not be made.

Of the test conditions, only one was useful for the calibration of the flat-wake-code prediction of sidewash velocity, and that was at $\mu = 0.29$. The rest were at very low advance ratios. It was noted that the rotor wake was strongly asymmetric where the downwash behind the advancing side of the rotor was greater than behind the retreating side. The rotor conditions were $C_T = 0.006$ and $\alpha = -4.2°$. The rotor propulsive force and torque coefficients are not provided in the reference, but the rotor was trimmed to zero flapping. The flow survey made with only the hub operating (i.e., no blades) showed that the hub contributes a substantial component of the lateral velocity in the vicinity of the vertical tail.

Presentation of Results

The results of this evaluation are presented in the following figures:

Discussion of Results

Correlation With Data From Reference 20

The calculated induced velocities of program DOWN should correspond to the analytical predictions of reference 20 since DOWN was meant to be the implementation of the analysis of reference 20. Figure 6 shows both data and predictions reproduced from reference 20. Figure 6 shows the azimuthal distribution of induced vertical velocity $\Delta\lambda$ at $\rho = 0.70$, $\mu = 0.15$, $C_T = 0.006$, and $y = -0.10$. According to reference 20, figure 6 shows satisfactory agreement between prediction and experimental data. It is also judged in reference 20 that using a circulation distribution that does not account for azimuthal variation fits better to the data than a circulation distribution that is a function of radius and azimuth.

Figure 7 shows a comparison of DOWN predictions (utilizing the three different circulations, with and without the azimuthal variation) with reference 20 data. DOWN predictions are for the linear circulation (fig. 7(a)), parabolic circulation (fig. 7(b)), and quartic circulation (fig. 7(c)). Of the distributions, the quartic distribution seems to provide the best fit, though only a fair fit, whereas the linear distribution fits best in the azimuth range from 135° to 240°. In the azimuth range from 330° to 30°, all predictions and those of reference 20 (shown in fig. 6) show peaks that do not fit well with the data. They likely show the effects of model mounting

apparatus on flow velocities. The azimuthal variation of circulation distribution does not improve the fit to the data.

Figures 8 and 9 present data from reference 20 where test conditions were $\mu = 0.15$, $C_T = 0.006$, and $y = -0.10$. The induced velocity $\Delta\lambda$ is plotted against ρ for various azimuth combinations. Where azimuths are greater than 180°, a negative range of ρ is used. The azimuth combinations of 0° and 180° (figs. 8(a) and 9(a)), 45° and 225° (figs. 8(b) and 9(b)), 90° and 270° (figs. 8(c) and 9(c)), and 135° and 315° (figs. 8(d) and 9(d)) are shown. Figure 8 compares DOWN predictions having the parabolic and quartic circulations with data from reference 20. Figure 9 compares DOWN predictions having the quartic circulation (with and without the azimuthal variation) with data from reference 20. (Recall that the notation m in the figures (e.g., G3m) indicates that an azimuthal variation of circulation is used in the prediction.) The results of DOWN for parabolic and quartic circulations appear to fit to the data, with the parabolic circulation being somewhat better in figure 8 than the quartic circulation. However, the fit is no better than that of figure 7. In figure 9, the use of an azimuthal variation of the quartic circulation did not improve the fit of prediction to data.

Figures 7, 8, and 9 do not show a clearly better correlation of DOWN predictions with one or the other of the circulation descriptions from the data of reference 20. This analysis was unable to reproduce the "good" agreement obtained in reference 20 (shown in fig. 6). Since the coding of DOWN is based on the guidance of reference 20, a closer fit of the DOWN prediction to the analysis of reference 20 should be expected. The results shown in reference 20 cannot be verified, whereas the code DOWN has been carefully checked. The poorest fit is in the azimuth range where rotor-hub wake effects must be significant.

Correlation With Data From References 24, 25, 26, 29, and 30

Comparisons of vertical induced velocity data of references 24, 25, 26, 29, and 30 (volumes I, II, III, VI, and VII, respectively) were made with the DOWN predictions and are presented in figures 10–14. Shown is the variation of induced flow $\Delta\lambda$ with azimuth ψ for three selected radial stations ($\rho = 0.60, 0.79$, and 0.98). The data shown have been corrected for the influence of the fuselage as defined in references 41 and 42. This correction process is demonstrated in figures 15 and 16 for $\mu = 0.15, 0.23$, and 0.30 and at radial stations of 0.60, 0.79, and 0.98. Figure 16 suggests that the experimental measurements are modestly affected by the presence of the fuselage as suggested by the analyses of reference 41.

Since there was no clear "best" circulation description for correlation with experimental data in figures 7, 8, and 9, and the quartic distribution appeared to be similar to patterns shown in reference 38, the quartic distribution was chosen for correlation of DOWN predictions with the data from references 24, 25, 26, 29, and 30. In general, the code provides a prediction of vertical inflow characteristics similar to that of experimental data as shown in figures 10–14. The data for the radial station 0.98 fitted best for $\psi = 90°$ to 270°, but with a significant difference in the azimuth range from 315° to 60°. That characteristic appears for the other radial stations of 0.60 and 0.79 as well (and in ref. 20). There are some other differences between predictions and data for these two stations. For example, in figures 11(a), 11(b), 12(a), and 12(b) there is significant upwash shown for the azimuth range from 60° to 150°, whereas the prediction shows downwash. The inaccuracy of velocity measurement is not enough to explain the difference. The hub wake effect on flow patterns to the rear and below the rotor would be even more significant. There are no data obtained in the tests cited in references 24 to 34 to provide an appraisal of such a hub wake effect. Even recently developed analytical tools (such as those of refs. 43 and 44) for rotorcraft interactional aerodynamics have yet to address that need. It does appear that accounting for azimuthal variation of the quartic circulation offers a modest improvement in correlation.

Figures 17–21 offer another way of comparing DOWN predictions with the data from references 24, 25, 26, 29, and 30, i.e., a three-dimensional format. The differences between prediction and data can provide an appreciation of the complete inflow as opposed to those shown in figures 10–14. An obvious difference is the upwash predicted on both sides of the rotor disk for a radius where $\rho > 1.0$ and for azimuth ranges from 60° to 90° and 270° to 300° which are not evident in the data. However, the predicted patterns do correlate with data in showing maximum downwash occurring in the rear portion of the rotor disk and skewed to the advancing blade side of the disk (azimuth range of 0° to 90°). That was not the case in a comparison of the predictions of the analytical method of reference 14 with the very same data, as concluded in reference 35. The results of reference 35 using CAMRAD (Comprehensive Analytical Model of Rotorcraft Aerodynamics and Dynamics)

have shown maximum downwash toward the retreating side of the rotor disk (ref. 14). Several other analytical methods reviewed in reference 36 had the same problem of predicting the largest values of induced inflow to be on the retreating side of the rotor disk, which is the opposite from that measured. So, it appears that DOWN is better than those analyses (CAMRAD, UTRC Rotorcraft Wake Analysis, and Beddoes) mentioned in references 35 and 36 in predicting the largest values of inflow on the retreating side of the rotor disk.

Correlation With Data From Reference 5

Several sets of data (all at $\mu = 0.232$) presented in reference 5 are used for correlation. The first set (fig. 22) provides for a correlation with the prediction of inflow in a plane $y \approx 0.18$ above the rotor tip path plane for $\mu = 0.232$. The several longitudinal stations shown are at $x = 1.0$, 0.5, 0, -0.5, and -1.07. The measurement height at several stations differed modestly from 0.18, but the correct height is noted on each plot. The predicted inflow patterns are in general agreement with the data although there is a greater downflow measured for $z < -0.5$. Figures 23 and 24 offer comparisons of inflow and wake characteristics, i.e., above and below the rotor at two longitudinal stations ($x = -0.50$ and -1.07, respectively). The $\Delta\lambda$ characteristics shown in figure 24 are at a longitudinal station representative of an empennage station ($x = -1.07$). Again, the predicted airflow characteristics are in general agreement with the data, but there is a greater disparity for $z < 0$.

Correlation With Data From Reference 37

The wake survey test data of reference 37 may be more representative of the airflow characteristic of a helicopter empennage location than that of reference 5 since there is a full representation of a fuselage with the resultant wake. The results of reference 37 indicate that the flow field is quite chaotic with a strong swirling flow, which appears to be mainly the influence of the rotor hub. The hub-alone data were subtracted from data for the rotor to obtain wake flow characteristics more appropriate for correlation (since flat wake theory does not address hub effects). In figures 25 (for sidewash $\Delta\eta$) and 26 (for downwash $\Delta\lambda$) the rotors with and without hub data are compared with the flat-wake-code predictions. The agreement between data and prediction is very poor. A reason may be that separated flow from the fuselage and engine nacelles is substantial and the resultant wake has a gross effect on patterns at the tail pylon. It is obvious that just subtracting hub-alone data from rotor-plus-hub data does not offer much improvement in correlation and there is a need for more sophisticated analyses, such as the free wake flow field analysis of reference 44 wherein a better correlation with data from reference 37 is achieved. However, the good correlation in reference 44 cannot be attributed to the incorporation of a hub and fuselage wake.

Concluding Remarks

An analysis of helicopter inflow-wake velocities called *flat wake theory* was implemented in a computer code. This code known as DOWN will predict the three orthogonal components of flow velocity in the field surrounding the rotor. The predictive capability of the coded versions of the theory was correlated with flow velocity data from several sources. These provide mostly vertical induced flow velocity measurements and some meager lateral induced flow information. The data used from these several sources are compromised by the significant influence of the hub and rotor drive system.

The assumptions that were made in the development of the flat rotor flow field analysis may well contribute to a disparity between data and prediction, and these are listed as follows: (1) the modeling of the classical helical vortex wake by a system of rectilinear vortices, (2) a rigid wake without interaction between induced velocities and wake structure, (3) an azimuthal average of circulation distribution on a rotor blade, (4) an azimuthal variation of circulation (and therefore no shed vorticity) not directly incorporated in the analysis, and (5) "bound" vorticity effects not represented.

In general, the coded version of flat wake theory provides vertical inflow patterns similar to experimental time-averaged measurements. Since the computer code was meant to be an implementation of an existing calculation scheme, it at least should have duplicated rotor flow calculations made for the calibration of the original presentation of the theory. That was not accomplished with the code DOWN. Since the code has been thoroughly checked by the developers, the original presentation of calibration needs verification.

Although several rotor blade circulation descriptions were used in the code in an attempt to bring about a better fit of prediction to measured vertical flow velocities, none were wholly satisfactory. Of these circulation patterns the one that is most like a flight test distribution is marginally best. Applying a factor to represent an azimuthal variation of circulation provided a modest improvement to the fit of predictions to some data. To some extent the disparities between prediction and data may be attributed

to rotor hub and fuselage wake effects that are not accounted for in the theory.

For the prediction of induced sidewash velocities in the vicinity of the helicopter tail, the paucity of data limited the attempted correlation of the code. The code predictions did not fit well with the data. However, the flow in that region is obviously dominated by the swirl effected by the rotor hub and the separated flow (i.e., wake) from the hub, pylon, and fuselage.

In spite of the evident disparities between data and DOWN predictions, the code predictions may be no worse than those of other analytical codes. For example, DOWN does predict greater downwash velocities on the advancing side of the rotor disk than on the retreating side which is not done by other analytical codes.

NASA Langley Research Center
Hampton, VA 23665-5225
March 5, 1992

References

1. Wheatley, John B.: *An Aerodynamic Analysis of the Autogiro Rotor With a Comparison Between Calculated and Experimental Results.* NACA Rep. 487, 1934.

2. Coleman, Robert P.; Feingold, Arnold M.; and Stempin, Carl W.: *Evaluation of the Induced-Velocity Field of an Idealized Helicopter Rotor.* NACA WR L-126, 1945. (Formerly NACA L5E10.)

3. Mangler, K. W.; and Squire, H. B.: *The Induced Velocity Field of a Rotor.* R. & M. No. 2642, British Aeronautical Research Council, May 1950.

4. Castles, Walter, Jr.; and De Leeuw, Jacob Henri: *The Normal Component of the Induced Velocity in the Vicinity of a Lifting Rotor and Some Examples of Its Application.* NACA Rep. 1184, 1954. (Supersedes NACA TN 2912.)

5. Heyson, Harry H.; and Katzoff, S.: *Induced Velocities Near a Lifting Rotor With Nonuniform Disk Loading.* NACA Rep. 1319, 1957. (Supersedes NACA TN 3690 by Heyson and Katzoff and TN 3691 by Heyson.)

6. Heyson, Harry H.: *A Note on the Mean Value of Induced Velocity for a Helicopter Rotor.* NASA TN D-240, 1960.

7. Heyson, Harry H.: *Equations for the Induced Velocities Near a Lifting Rotor With Nonuniform Azimuthwise Vorticity Distribution.* NASA TN D-394, 1960.

8. Scully, Michael P.: Computation of Helicopter Rotor Wake Geometry and Its Influence on Rotor Harmonic Airloads. Ph.D. Thesis, Massachusetts Inst. of Technology, Feb. 1975.

9. Egolf, T. Alan; and Landgrebe, Anton J.: *Helicopter Rotor Wake Geometry and Its Influence in Forward Flight. Volume I—Generalized Wake Geometry and Wake Effect on Rotor Airloads and Performance.* NASA CR-3726, 1983.

10. Peters, David A.; and He, Cheng Jian: A Closed-Form Unsteady Aerodynamic Theory for Lifting Rotors in Hover and Forward Flight. *43rd Annual Forum Proceedings, Volume II,* American Helicopter Soc., 1987, pp. 839–865.

11. Peters, David A.; and He, Cheng Jian: Comparison of Measured Induced Velocities With Results From a Closed-Form Finite State Wake Model in Forward Flight. *45th Annual Forum Proceedings,* American Helicopter Soc., 1989, pp. 533–550.

12. Bliss, Donald B.; and Miller, Wayne O.: Efficient Free Wake Calculations Using Analytical/Numerical Matching and Far-Field Linearization. *45th Annual Forum Proceedings,* American Helicopter Soc., 1989, pp. 253–263.

13. Miller, Wayne O.; and Bliss, Donald B.: Direct Periodic Solutions of Rotor Free Wake Calculations by Inversion of a Linear Periodic System. *46th Annual Forum Proceedings, Volume II,* American Helicopter Soc., 1990, pp. 757–769.

14. Johnson, Wayne: *A Comprehensive Analytical Model of Rotorcraft Aerodynamics and Dynamics. Part I: Analysis Development.* NASA TM-81182, USAAVRADCOM TR-80-A-5, 1980.

15. Johnson, Wayne: *Helicopter Theory.* Princeton Univ. Press, c.1980.

16. Ormiston, Robert A.: An Actuator Disc Theory for Rotor Wake Induced Velocities. *Aerodynamics of Rotary Wings,* AGARD-CP-111, 1972, pp. 2-1–2-19.

17. Chen, Robert T. N.: A Survey of Nonuniform Inflow Models for Rotorcraft Flight Dynamics and Control Applications. *Vertica,* vol. 14, no. 2, 1990, pp. 147–184.

18. Zhao, Xin; and Curtiss, H. C.: A Linearized Model of Helicopter Dynamics Including Correlation With Flight Test. *Proceedings of the 2nd. International Conference on Rotorcraft Basic Research,* Univ. of Maryland and American Helicopter Soc., 1988, pp. ZHAO-1–ZHAO-14.

19. Prouty, R. W.: Importance of Aerodynamics on Handling Qualities. *National Specialists' Meeting on Aerodynamics and Aeroacoustics—Proceedings,* American Helicopter Soc., 1987.

20. Baskin, V. E.; Vil'dgrube, L. S.; Vozhdayev, Ye. S.; and Maykapar, G. I.: *Theory of the Lifting Airscrew.* NASA TT F-823, 1976.

21. Stepniewski, W. Z.: *Rotary-Wing Aerodynamics. Volume I—Basic Theories of Rotor Aerodynamics (With Application to Helicopter).* NASA CR-3082, 1979.

22. Vil'dgrube, L. S. (W. Z. Stepniewski and W. L. Metz, transl. and eds.): *Helicopters (Vertolety)—Calculations of Integral Aerodynamic Characteristics and Flight-Mechanics Data.* FSTC-HT-659-85, U.S. Army, 1977.

23. Wilson, John C.: *User's Guide for a "Flat Wake" Rotor Inflow/Wake Velocity Prediction Code, "DOWN."* NASA TM-104139, AVSCOM TR-91-B-016, 1991.

24. Elliott, Joe W.; Althoff, Susan L.; and Sailey, Richard H.: *Inflow Measurement Made With a Laser Velocimeter on a Helicopter Model in Forward Flight. Volume I—Rectangular Planform Blades at an Advance Ratio of 0.15.* NASA TM-100541, AVSCOM TM-88-B-004, 1988.

25. Elliott, Joe W.; Althoff, Susan L.; and Sailey, Richard H.: *Inflow Measurement Made With a Laser Velocimeter on a Helicopter Model in Forward Flight. Volume II—Rectangular Planform Blades at an Advance Ratio of 0.23.* NASA TM-100542, AVSCOM TM-88-B-005, 1988.

26. Elliott, Joe W.; Althoff, Susan L.; and Sailey, Richard H.: *Inflow Measurement Made With a Laser Velocimeter on a Helicopter Model in Forward Flight. Volume III—Rectangular Planform Blades at an Advance Ratio of 0.30.* NASA TM-100543, AVSCOM TM-88-B-006, 1988.

27. Elliott, Joe W.; Althoff, Susan L.; and Sailey, Richard H.: *Inflow Measurement Made With a Laser Velocimeter on a Helicopter Model in Forward Flight. Volume IV—Tapered Planform Blades at an Advance Ratio of 0.15.* NASA TM-100544, AVSCOM TM-88-B-007, 1988.

28. Elliott, Joe W.; Althoff, Susan L.; and Sailey, Richard H.: *Inflow Measurements Made With a Laser Velocimeter on a Helicopter Model in Forward Flight. Volume V—Tapered Planform Blades at an Advance Ratio of 0.23.* NASA TM-100545, AVSCOM TM-88-B-008, 1988.

29. Hoad, Danny R.; Althoff, Susan L.; Elliott, Joe W.; and Sailey, Richard H.: *Inflow Measurements Made With a Laser Velocimeter on a Helicopter Model in Forward Flight. Volume VI: Rectangular Planform Blades at an Advance Ratio of 0.35.* NASA TM-101598, AVSCOM TM-89-B-001, 1989.

30. Hoad, Danny R.; Althoff, Susan L.; Elliott, Joe W.; and Sailey, Richard H.: *Inflow Measurements Made With a Laser Velocimeter on a Helicopter Model in Forward Flight. Volume VII: Rectangular Planform Blades at an Advance Ratio of 0.40.* NASA TM-101599, AVSCOM TM-89-B-002, 1989.

31. Althoff, Susan L.; Elliott, Joe W.; Hoad, Danny R.; and Sailey, Richard H.: *Inflow Measurements Made With a Laser Velocimeter on a Helicopter Model in Forward Flight. Volume VIII: Rectangular Planform Blades at an Advance Ratio of 0.23, 0.50 Chord Above the Tip Path Plane.* NASA TM-102642, AVSCOM TM-90-B-007, 1990.

32. Althoff, Susan L.; Elliott, Joe W.; Hoad, Danny R.; and Sailey, Richard H.: *Inflow Measurements Made With a Laser Velocimeter on a Helicopter Model in Forward Flight. Volume IX: Rectangular Planform Blades at an Advance Ratio of 0.23, 0.75 Chord Above the Tip Path Plane.* NASA TM-102643, AVSCOM TM-90-B-008, 1990.

33. Althoff, Susan L.; Elliott, Joe W.; Hoad, Danny R.; and Sailey, Richard H.: *Inflow Measurements Made With a Laser Velocimeter on a Helicopter Model in Forward Flight. Volume X: Rectangular Planform Blades at an Advance Ratio of 0.30, 0.50 Chord Above the Tip Path Plane.* NASA TM-102644, AVSCOM TM-90-B-009, 1990.

34. Althoff, Susan L.; Elliott, Joe W.; Hoad, Danny R.; and Sailey, Richard H.: *Inflow Measurements Made With a Laser Velocimeter on a Helicopter Model in Forward Flight. Volume XI: Rectangular Planform Blades at an Advance Ratio of 0.30, 0.73 Chord Above the Tip Path Plane.* NASA TM-102645, AVSCOM TM-90-B-010, 1990.

35. Hoad, Danny R.: *Rotor Induced-Inflow-Ratio Measurements and CAMRAD Calculations.* NASA TP-2946, AVSCOM TM-89-B-010, 1990.

36. Hoad, Danny R.; Althoff, Susan L.; and Elliott, Joe W.: Rotor Inflow Variability With Advance Ratio. *44th Annual Forum Proceedings,* American Helicopter Soc., c.1988, pp. 57–72.

37. Logan, A. H.; Prouty, R. W.; and Clark, D. R.: *Wind Tunnel Tests of Large- and Small-Scale Rotor Hubs and Pylons.* USAAVRADCOM-TR-80-D-21, U.S. Army, Apr. 1981. (Available from DTIC as AD A098 510.)

38. Johnson, Wayne: Airloads and Wake Models for a Comprehensive Helicopter Analysis. *Vertica,* vol. 14, no. 3, 1990, pp. 255–300.

39. Gentry, Garl L., Jr.; Quinto, P. Frank; Gatlin, Gregory M.; and Applin, Zachary T.: *The Langley 14- by 22-Foot Subsonic Tunnel: Description, Flow Characteristics, and Guide for Users.* NASA TP-3008, 1990.

40. Phelps, Arthur E., III; and Berry, John D.: *Description of the U.S. Army Small-Scale 2-Meter Rotor Test System.* NASA TM-87762, AVSCOM TM-86-B-4, 1987.

41. Berry, John D.; and Althoff, Susan L.: *Computing Induced Velocity Perturbations Due to a Helicopter Fuselage in a Free Stream.* NASA TM-4113, AVSCOM TR-89-B-001, 1989.

42. Berry, John D.; and Althoff, Susan L.: Inflow Velocity Pertubations Due to Fuselage Effects in the Presence of a Fully Interactive Wake. *46th Annual Forum Proceedings, Volume II,* American Helicopter Soc., 1990, pp. 1111–1120.

43. Quackenbush, T. R.; Bliss, D. B.; Lam, C-M. G.; and Katz, A.: New Vortex/Surface Interaction Methods for the Prediction of Wake-Induced Airframe Loads. *46th Annual Forum Proceedings, Volume II,* American Helicopter Soc., 1990, pp. 1099–1110.

44. Quackenbush, Todd R.; and Bliss, Donald B.: Free Wake Flow Field Calculations for Rotorcraft Interactional Aerodynamics. *Vertica,* vol. 14, no. 3, 1990, pp. 313–327.

Table I. Test Conditions of Experimental Data

(a) Data from references 20, 24, 25, 26, 29, and 30

Reference	μ	C_T	y	ρ	ψ, deg	α, deg
20	0.150	0.0060	−0.100	0.7	Range	(a)
24	.149	.0063	.077	Range	↓	−3.00
25	.230	.0065	↓	↓	↓	−3.04
26	.300	.0065	↓	↓	↓	−4.04
29	.350	.0064	↓	↓	↓	−5.70
30	.400	.0064	↓	↓	↓	−5.70

[a]Not applicable.

(b) Data from references 5 and 37

Reference	μ	C_T	y	x	z	α, deg
5	0.232	0.00321	0.19/−0.23	1.0, 0.5, 0, −0.5, −1.07	Range	−9.50
37	0.290	0.006	−0.22/−0.51	−1.76	Range	−4.20

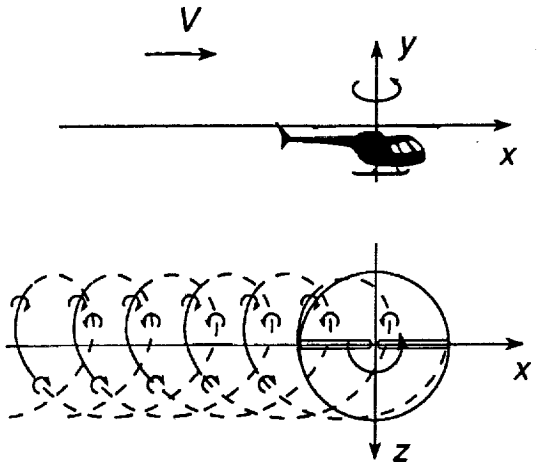

Figure 1. Flat wake formed by tip vortices of a rotor.

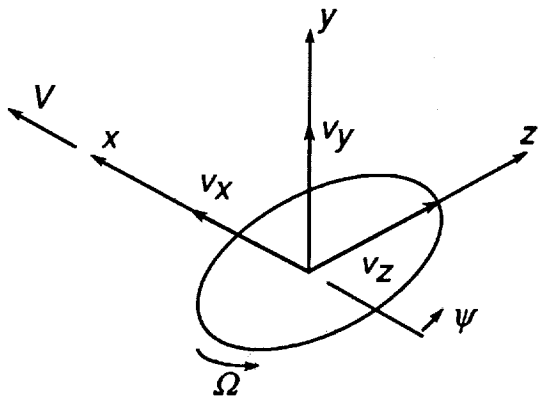

Figure 2. Coordinate system maintained from reference 20. Note that it differs from convention used in the U.S.

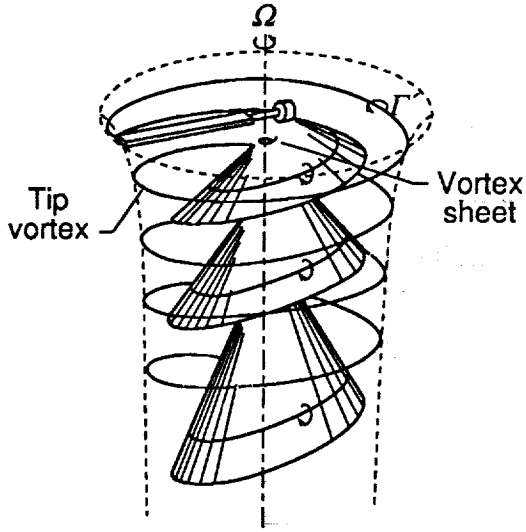

Figure 3. Rotor vorticity distribution in hover.

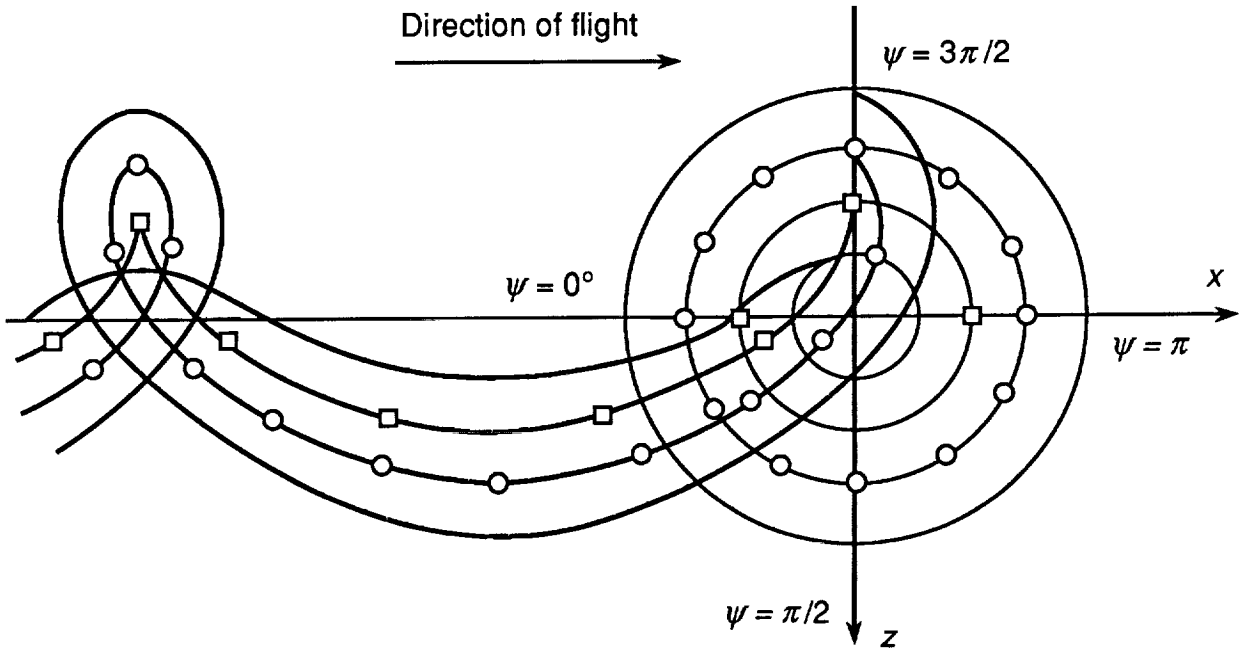

(a) Classical model of helical vortex wake structure for a rotor.

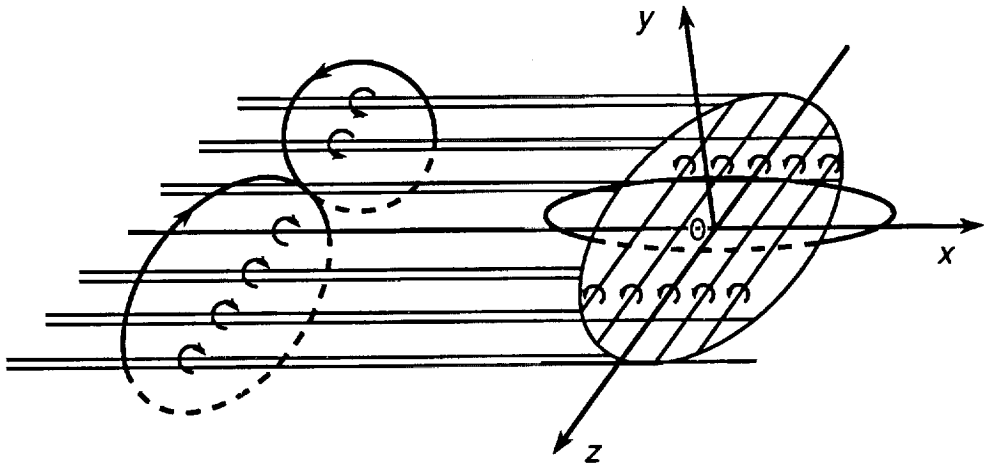

(b) Flat wake vortex system used in the theory.

Figure 4. Comparison of cycloidal vortex pattern and the equivalent rectilinear vortex system.

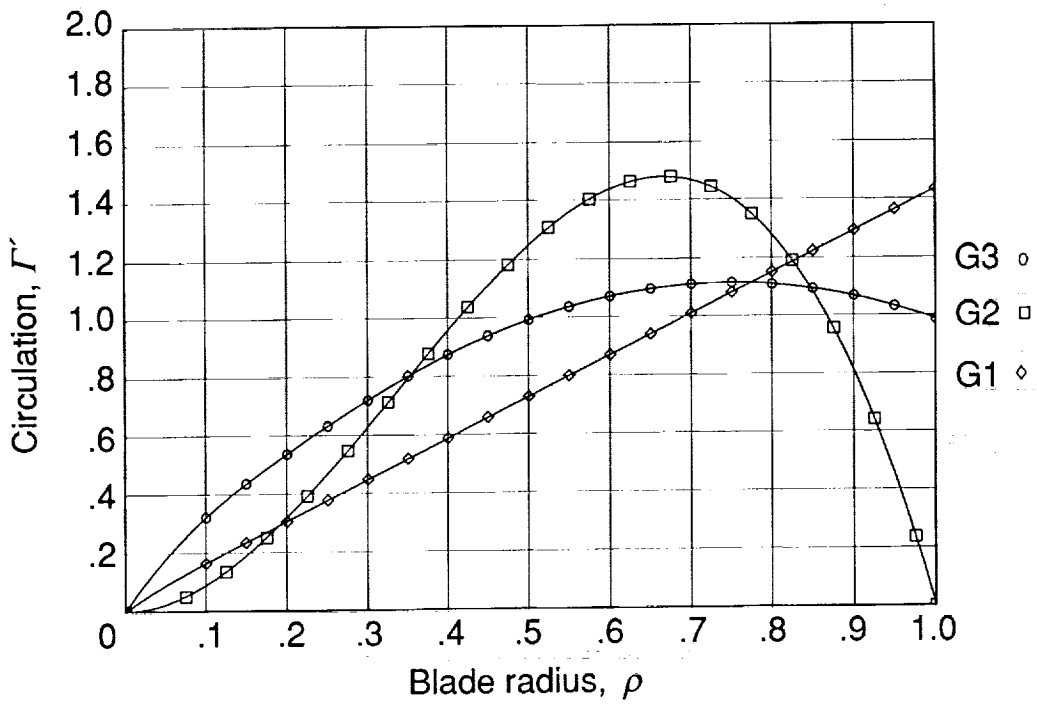

Figure 5. Linear (G1), parabolic (G2), and quartic (G3) circulation distributions used in DOWN for flow field predictions.

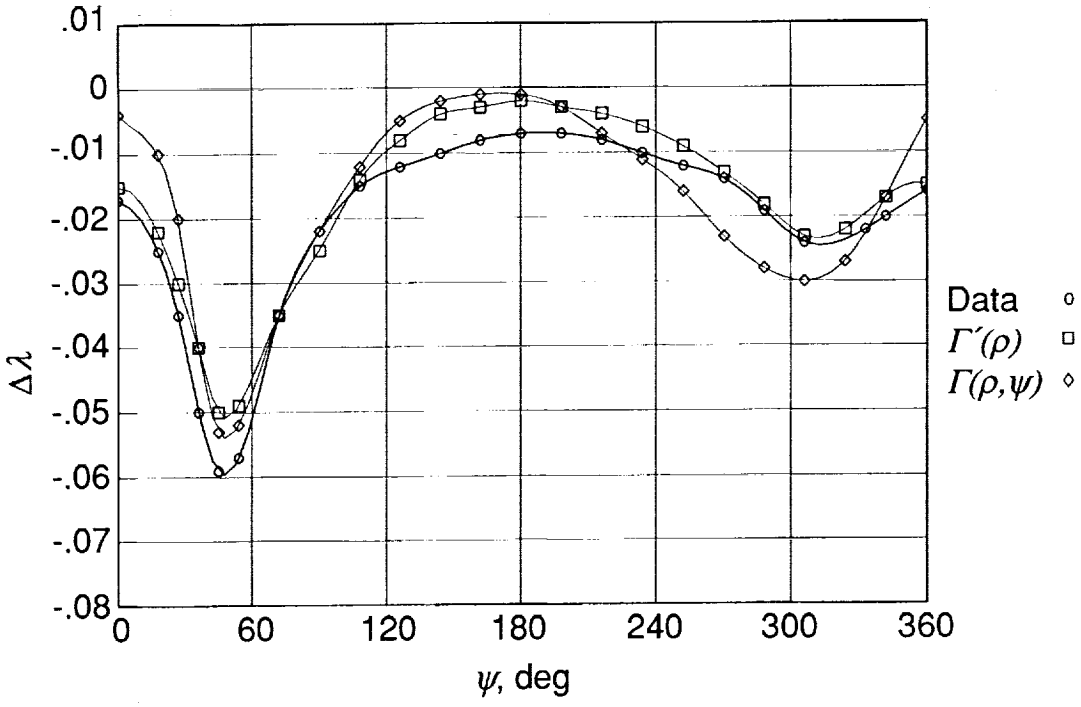

Figure 6. Data and flat wake predictions taken from figure 2.31 of reference 20 with circulation as a function of ρ, $\Gamma'(\rho)$, and as a function of ρ and ψ, $\Gamma(\rho, \psi)$. $\mu = 0.15$; $C_T = 0.006$; $y = -0.10$; $\rho = 0.70$.

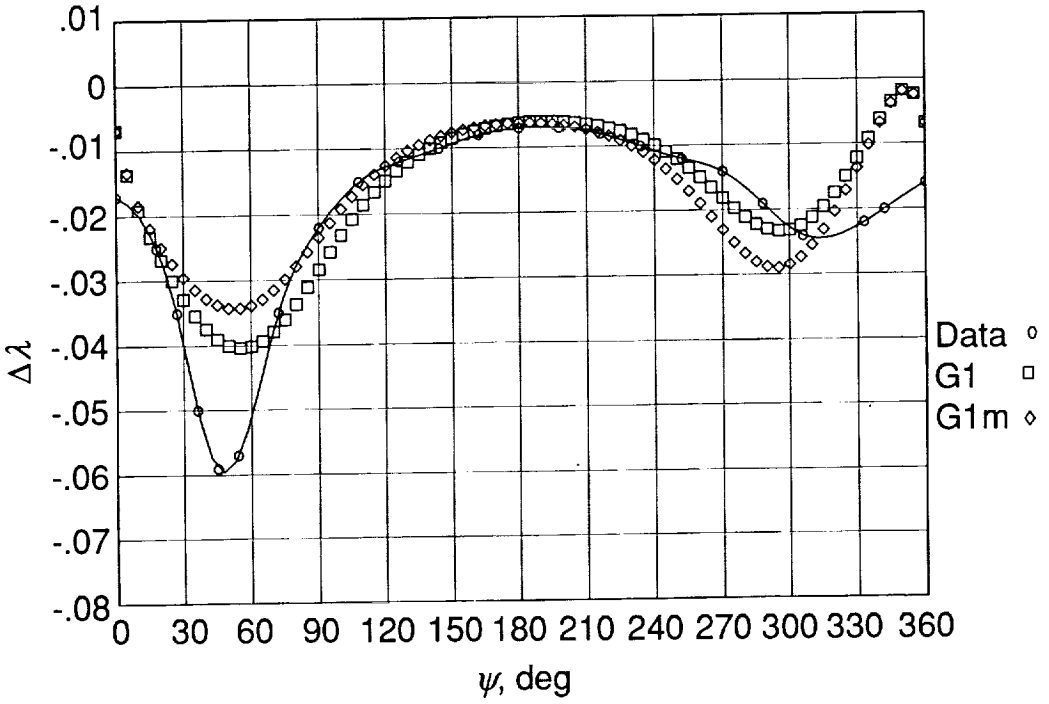

(a) Linear circulation with and without azimuthal variation.

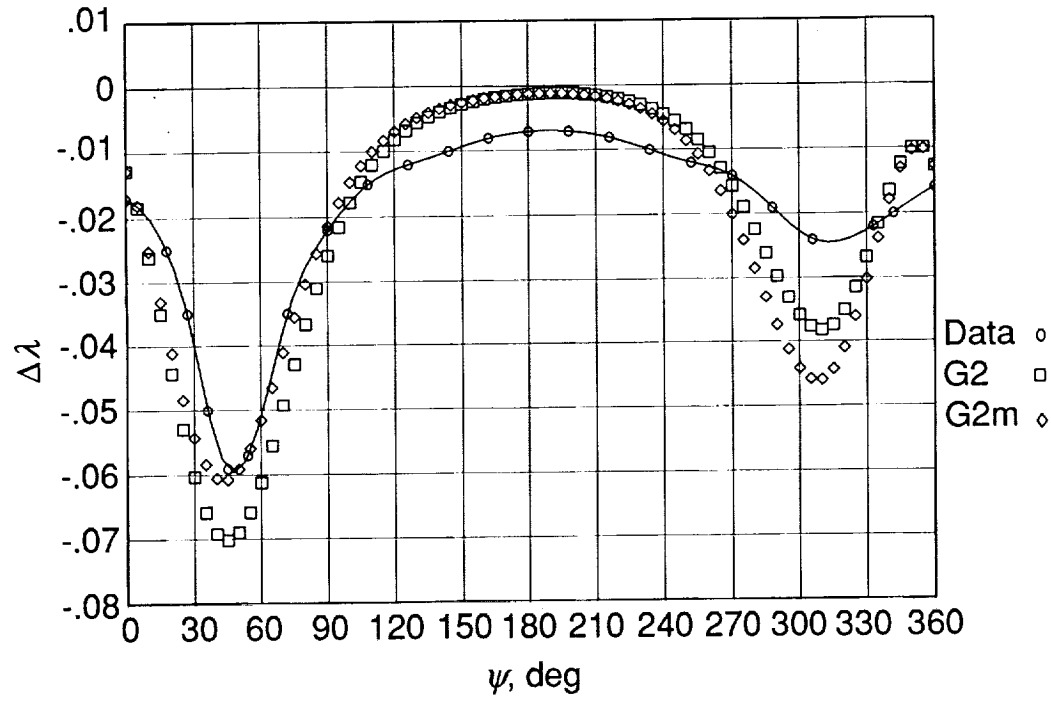

(b) Parabolic circulation with and without azimuthal variation.

Figure 7. Correlation of DOWN prediction with various circulation distributions of $\Delta\lambda$ with data of reference 20. $\mu = 0.15$; $C_T = 0.006$; $\rho = 0.7$; $y = -0.10$.

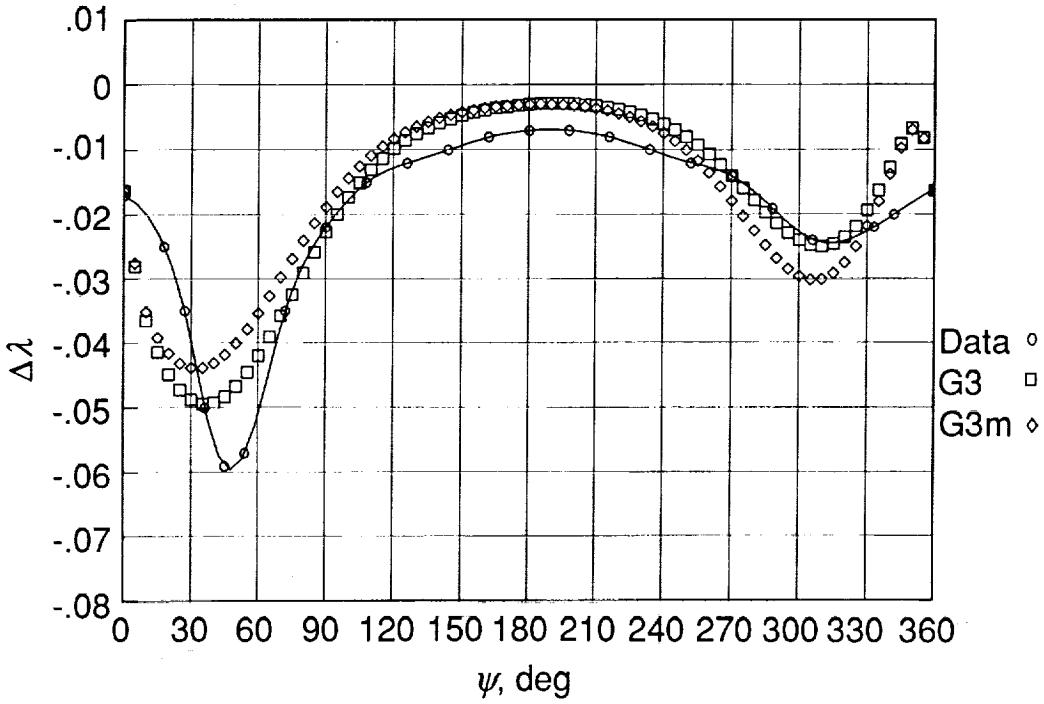

(c) Quartic circulation with and without azimuthal variation.

Figure 7. Concluded.

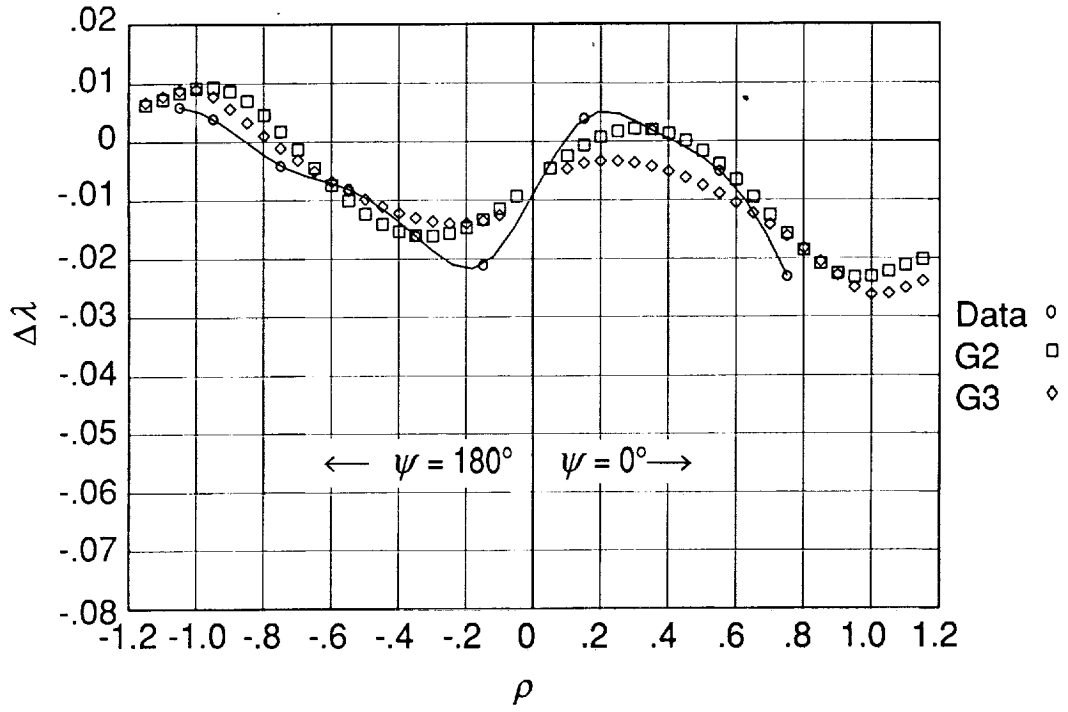

(a) $\psi = 0°$ and $180°$.

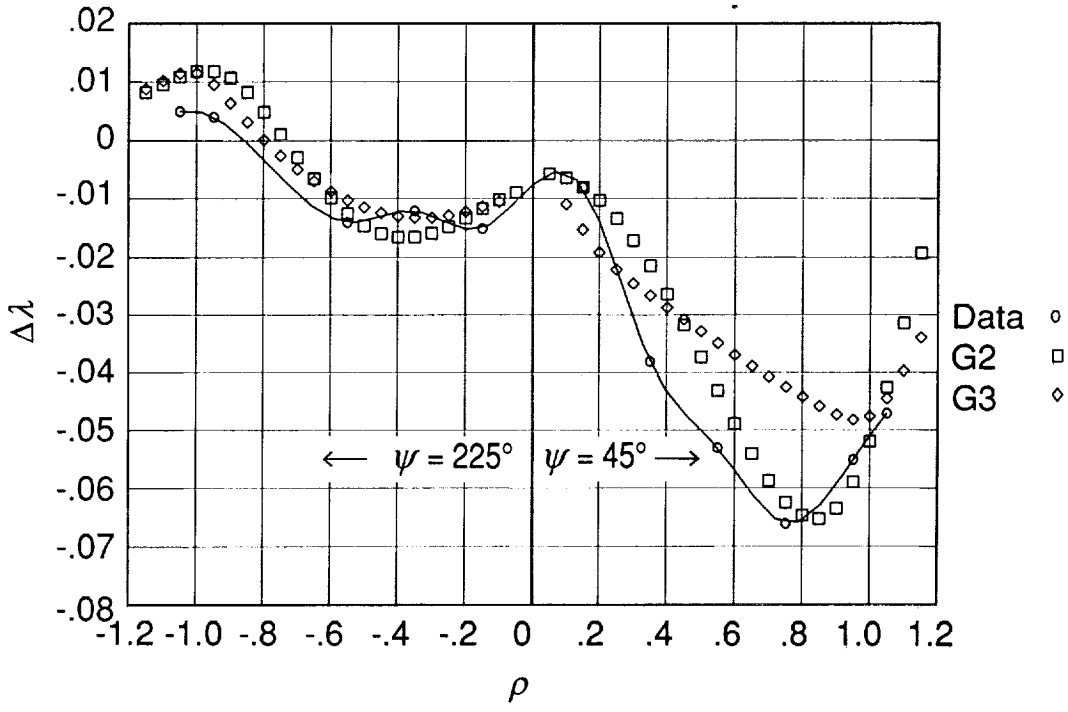

(b) $\psi = 45°$ and $225°$.

Figure 8. Correlation of DOWN prediction of $\Delta\lambda$ with data of reference 20 by using the parabolic and quartic circulations for various azimuthal angles. $\mu = 0.15$; $C_T = 0.006$; $y = -0.10$.

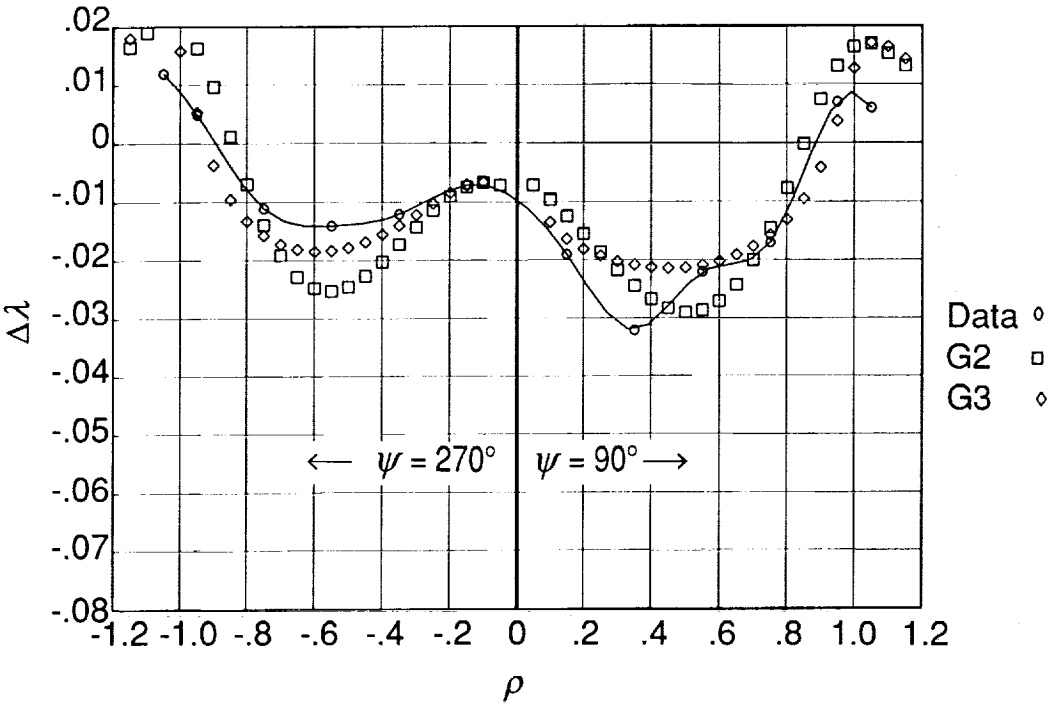

(c) $\psi = 90°$ and 270°.

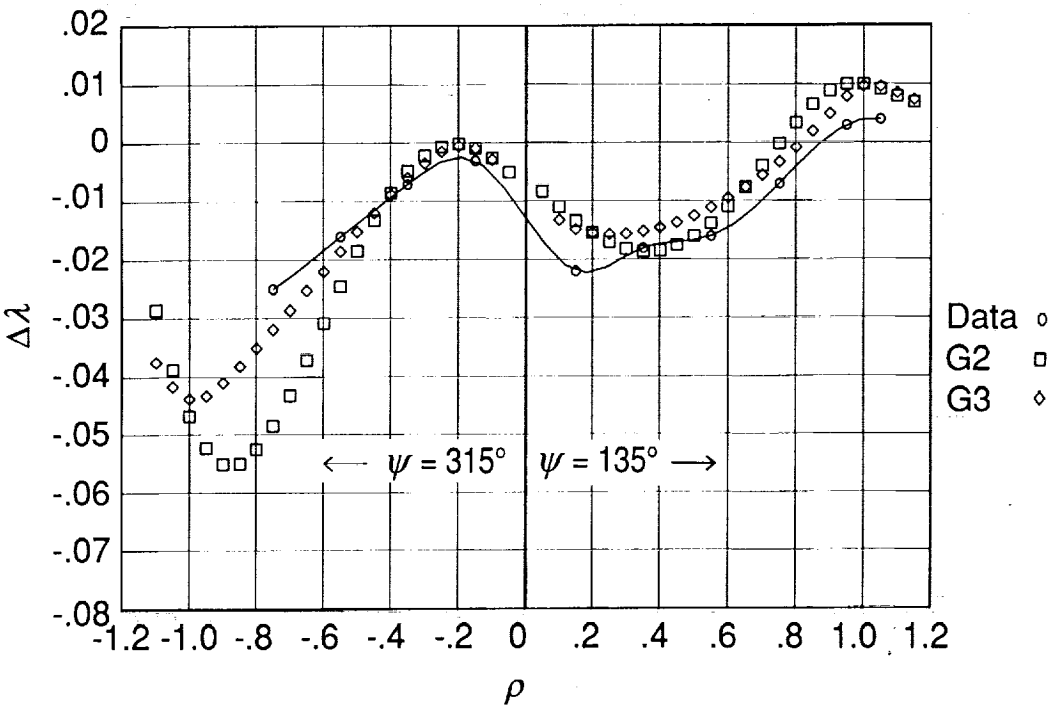

(d) $\psi = 135°$ and 315°.

Figure 8. Concluded.

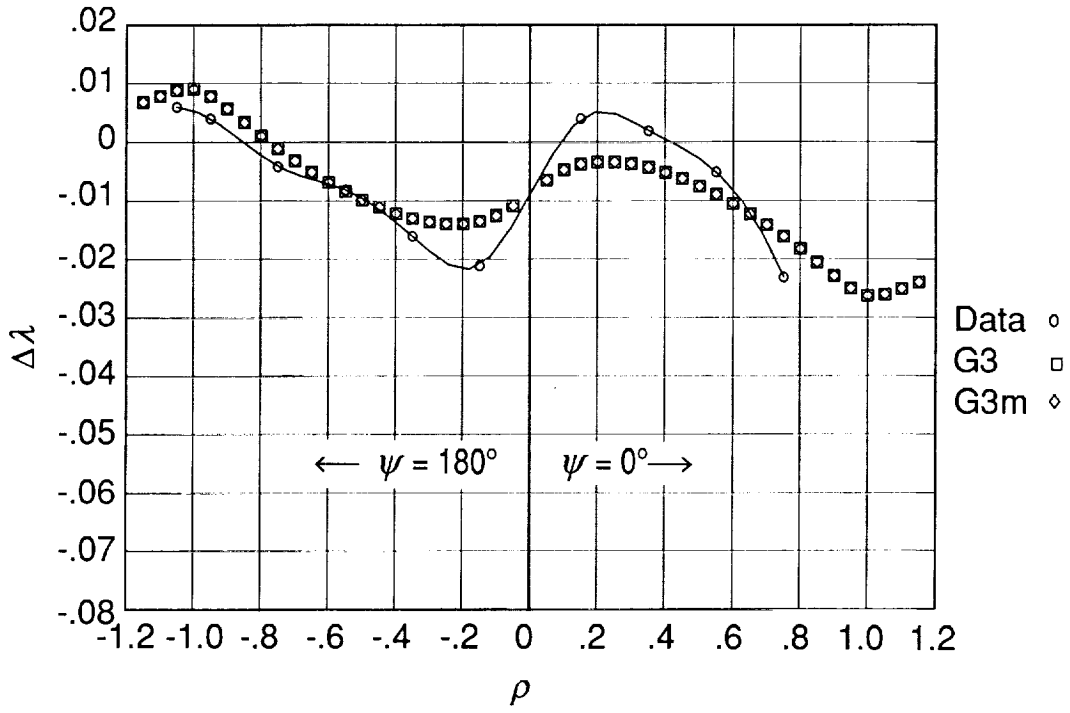

(a) $\psi = 0°$ and 180°.

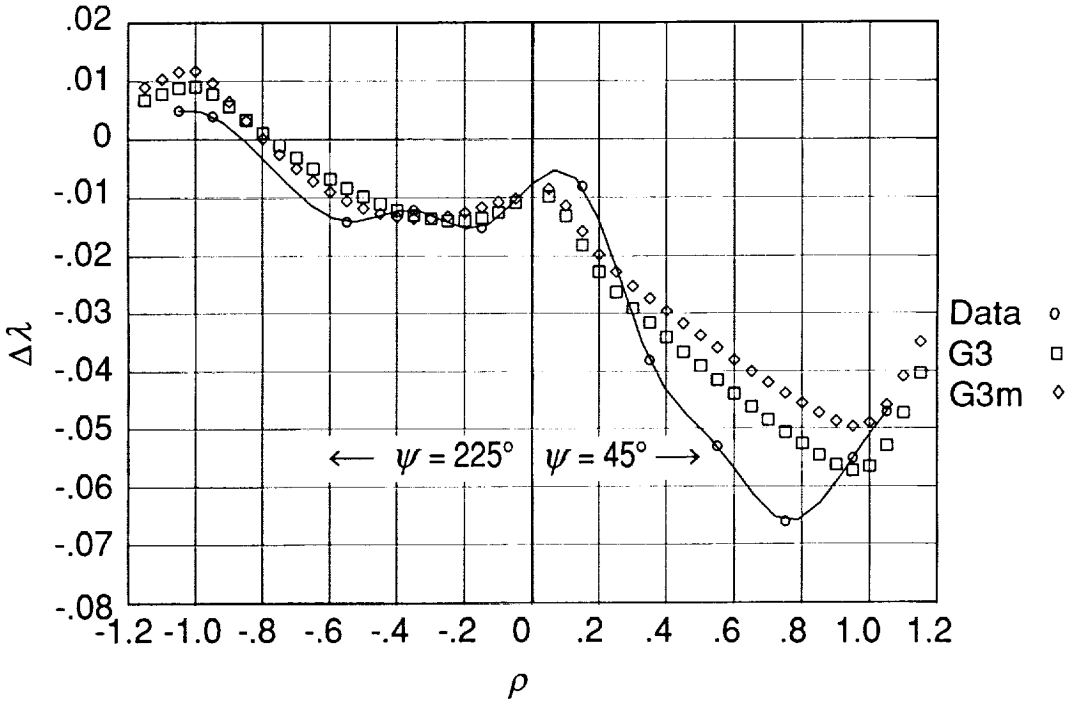

(b) $\psi = 45°$ and 225°.

Figure 9. Correlation of DOWN prediction of $\Delta\lambda$ with data of reference 20 by using the quartic circulation with and without the azimuthal variation of circulation. $\mu = 0.15$; $C_T = 0.006$; $y = -0.10$.

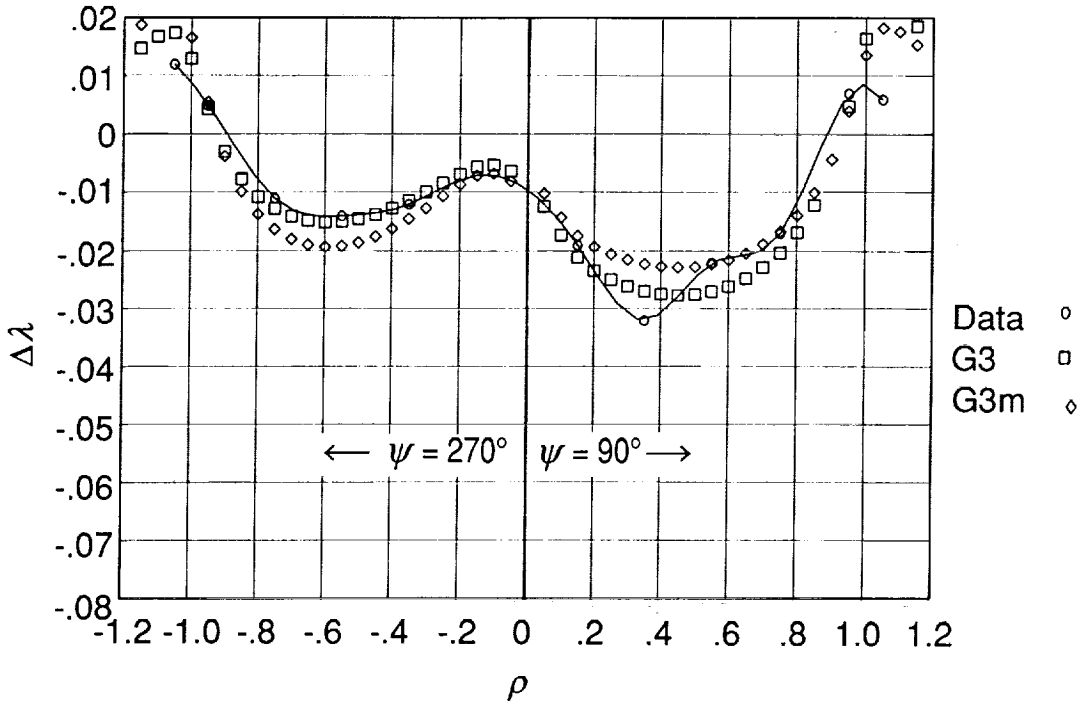

(c) $\psi = 90°$ and 270°.

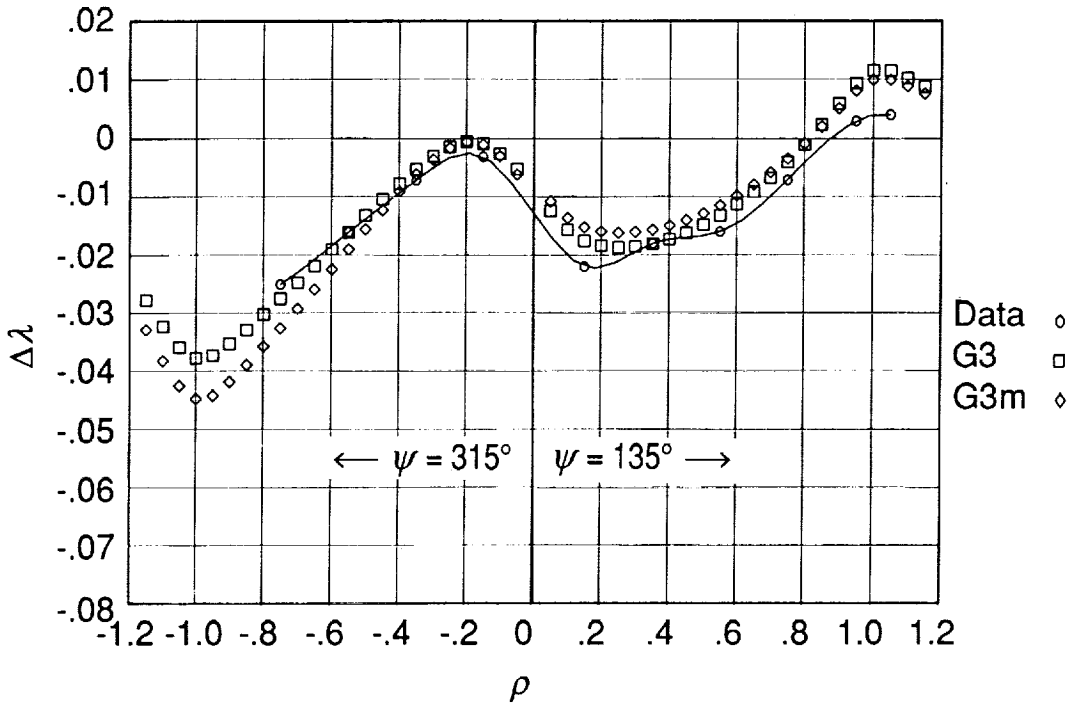

(d) $\psi = 135°$ and 315°.

Figure 9. Concluded.

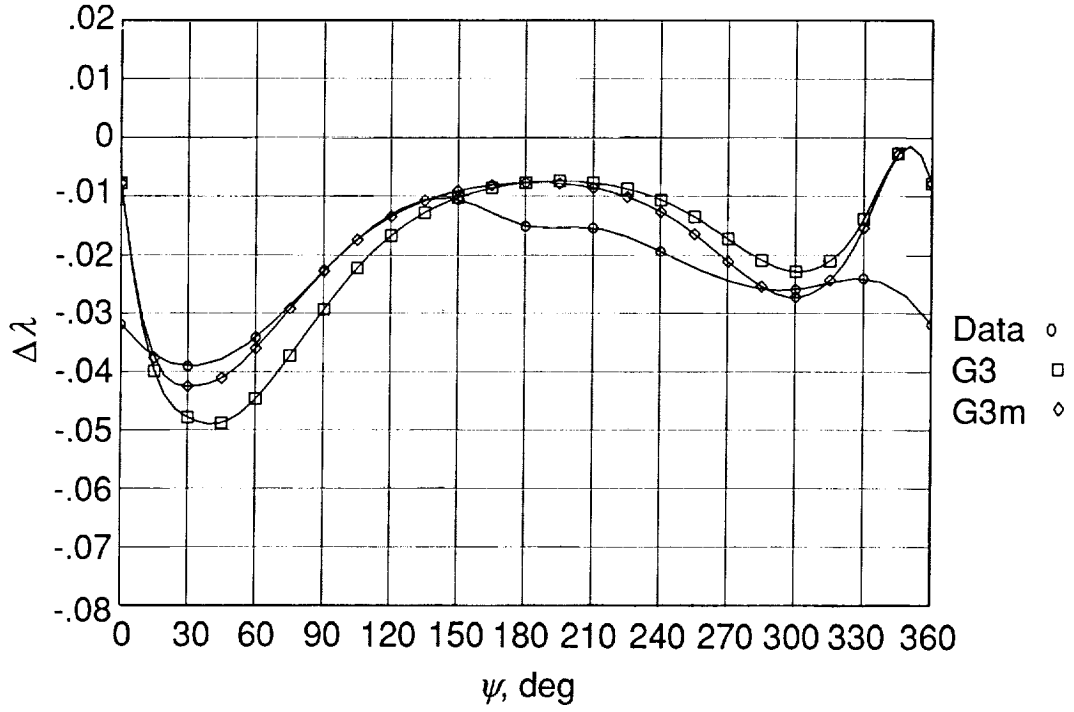

(a) $\rho = 0.60$.

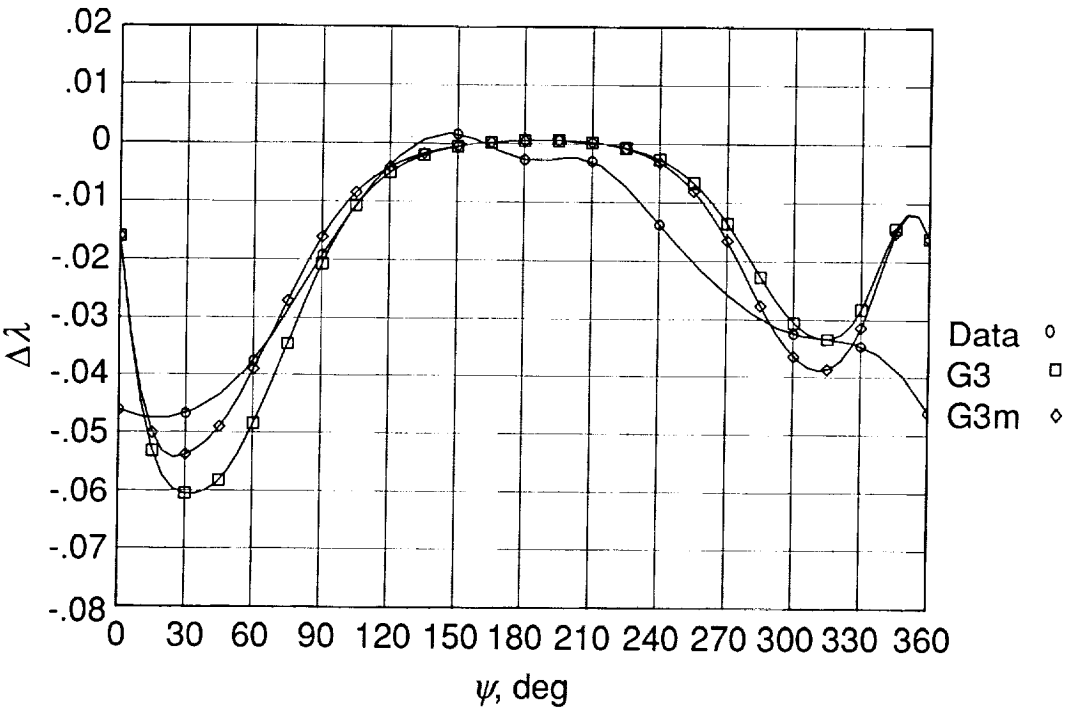

(b) $\rho = 0.79$.

Figure 10. Correlation of DOWN prediction of $\Delta\lambda$ with data of reference 24 by using quartic circulation with and without azimuthal variation of circulation. $\mu = 0.149$; $C_T = 0.0063$; $y = 0.077$.

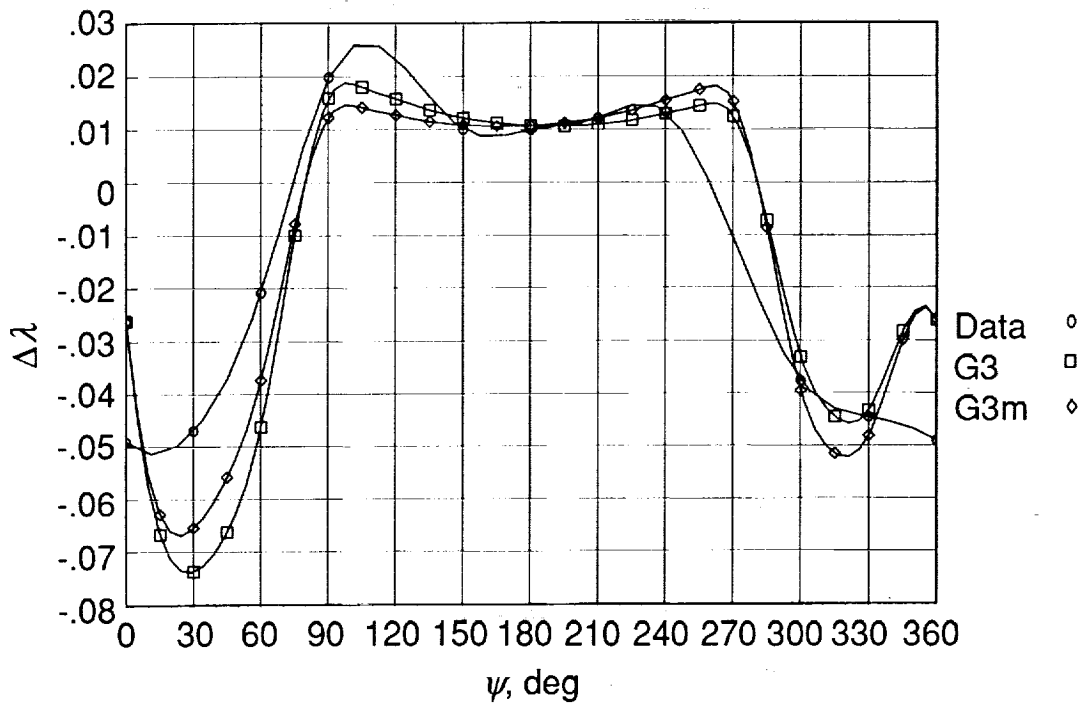

(c) $\rho = 0.98$.

Figure 10. Concluded.

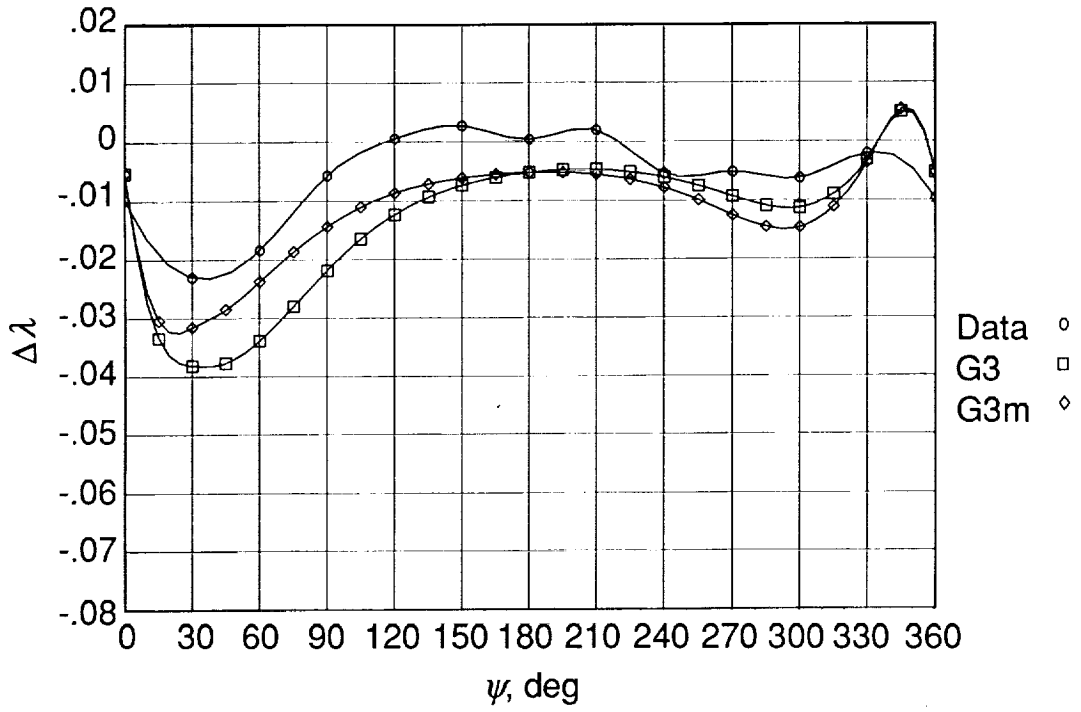

(a) $\rho = 0.60$.

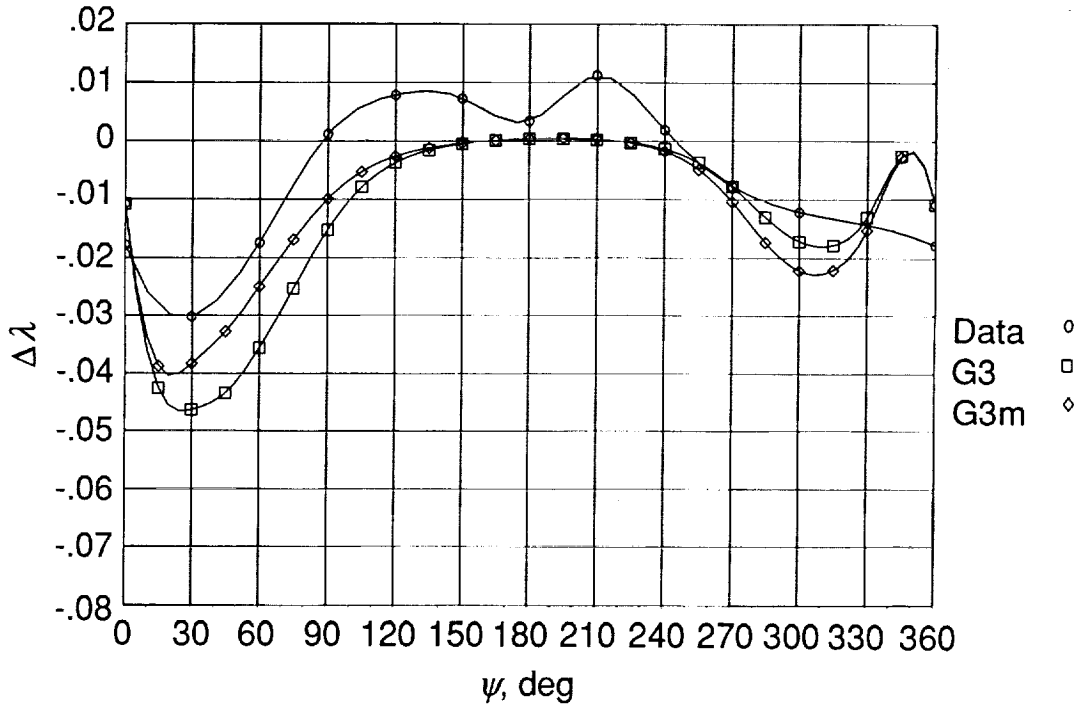

(b) $\rho = 0.79$.

Figure 11. Correlation of DOWN prediction of $\Delta\lambda$ with data of reference 25 by using the quartic circulation distribution with and without azimuthal variation of circulation. $\mu = 0.230$; $C_T = 0.0065$; $y = 0.077$.

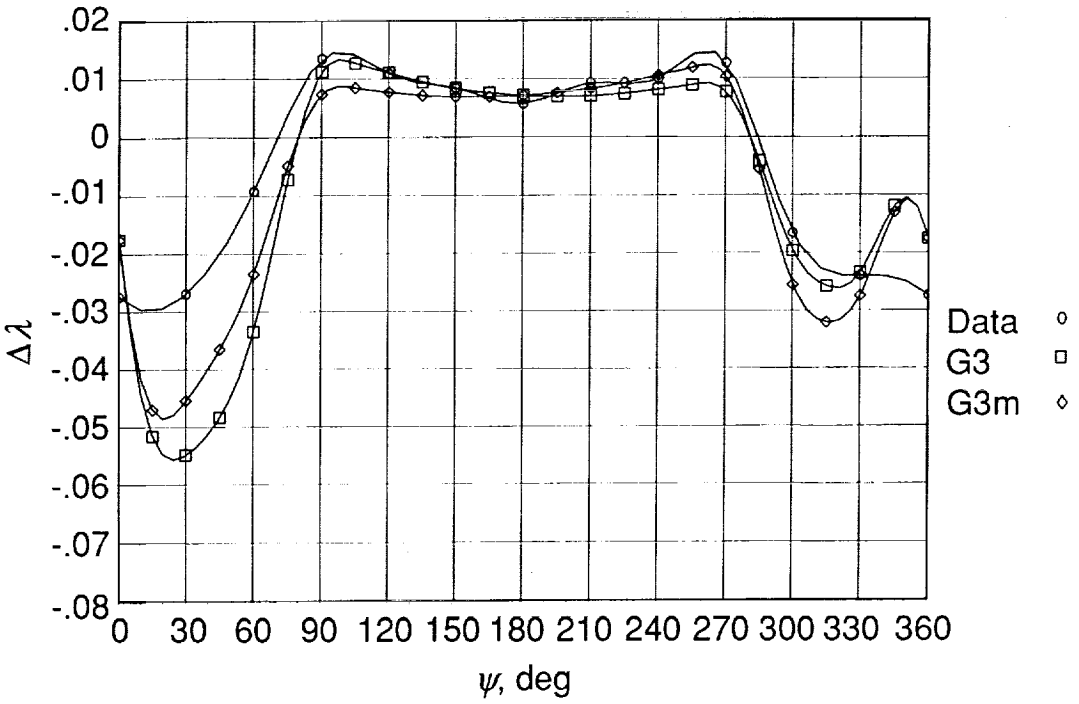

(c) $\rho = 0.98$.

Figure 11. Concluded.

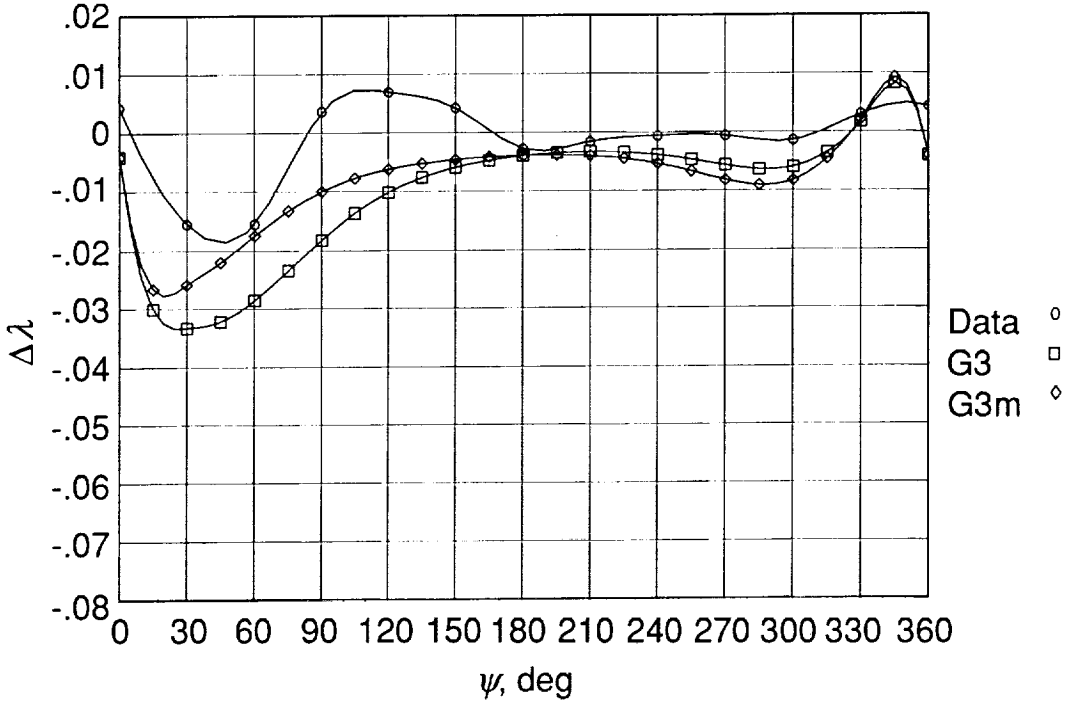

(a) $\rho = 0.60$.

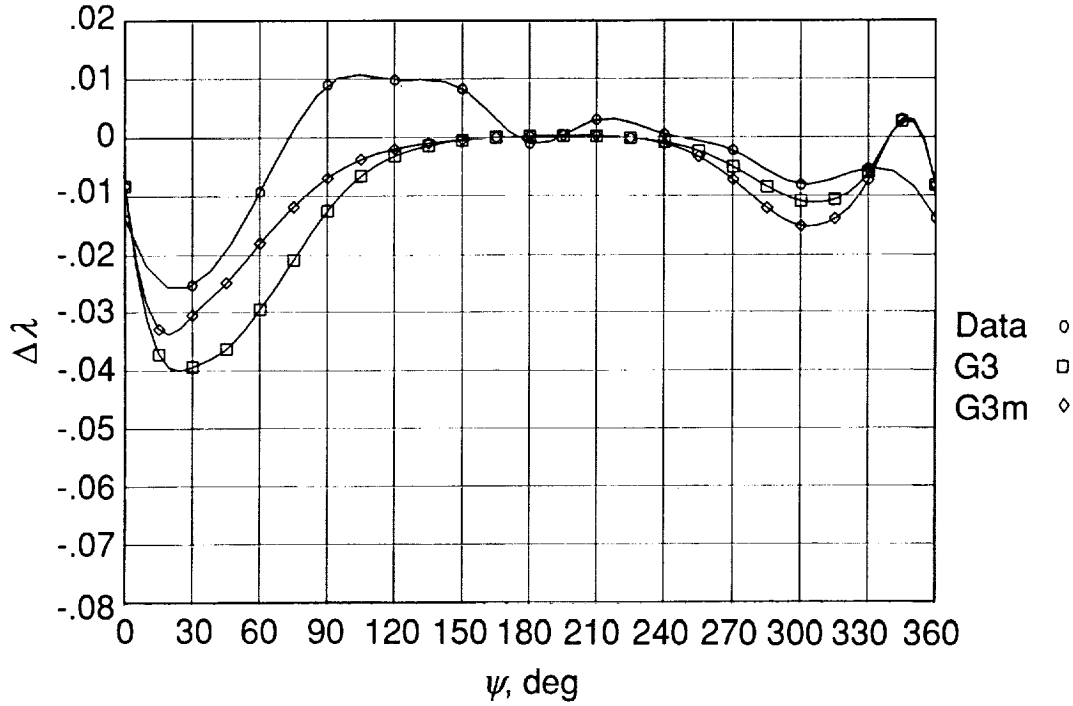

(b) $\rho = 0.79$.

Figure 12. Correlation of DOWN prediction of $\Delta\lambda$ with data of reference 26 by using the quartic circulation distribution with and without azimuthal variation of circulation. $\mu = 0.300$; $C_T = 0.00649$; $y = 0.077$.

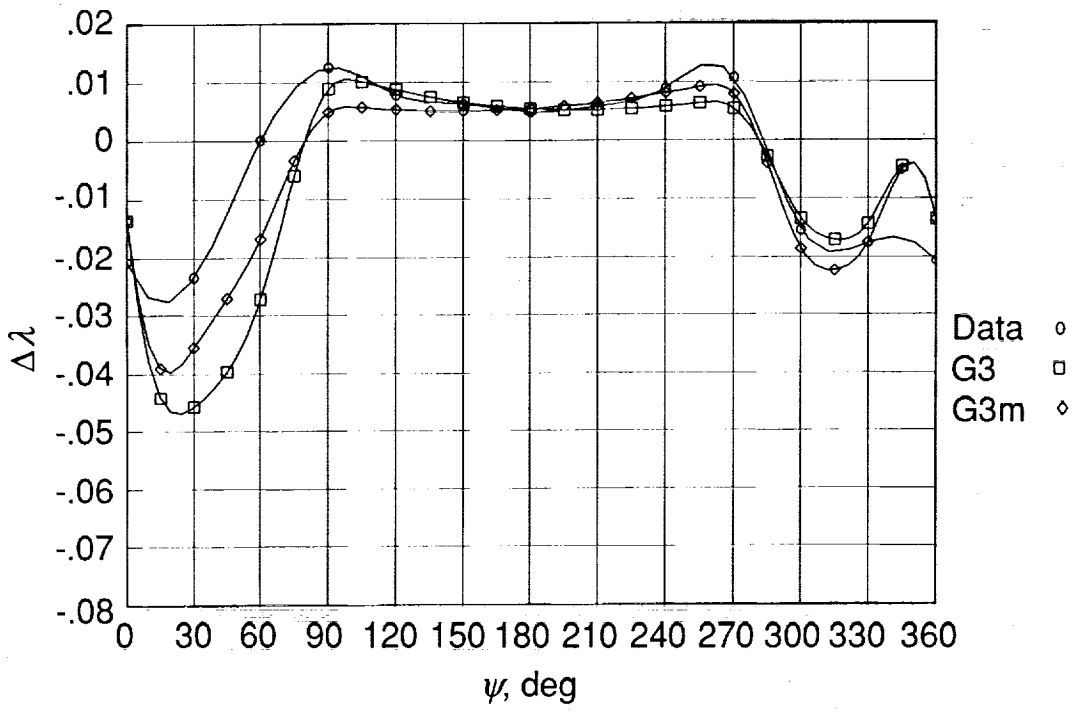

(c) $\rho = 0.98$.

Figure 12. Concluded.

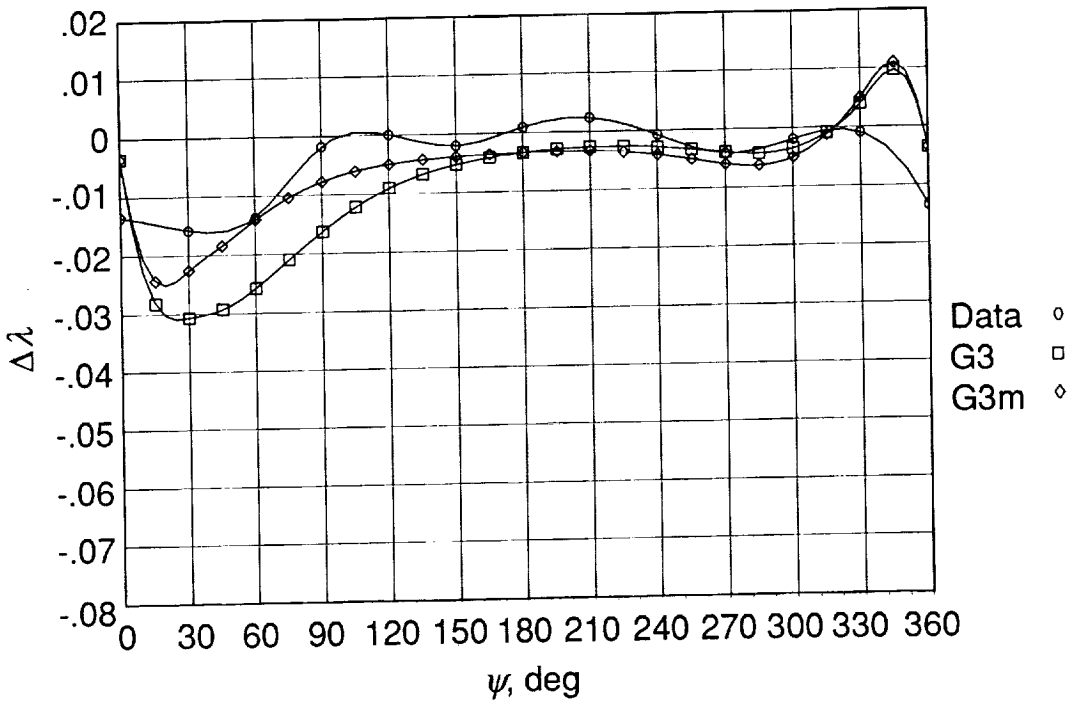

(a) $\rho = 0.60$.

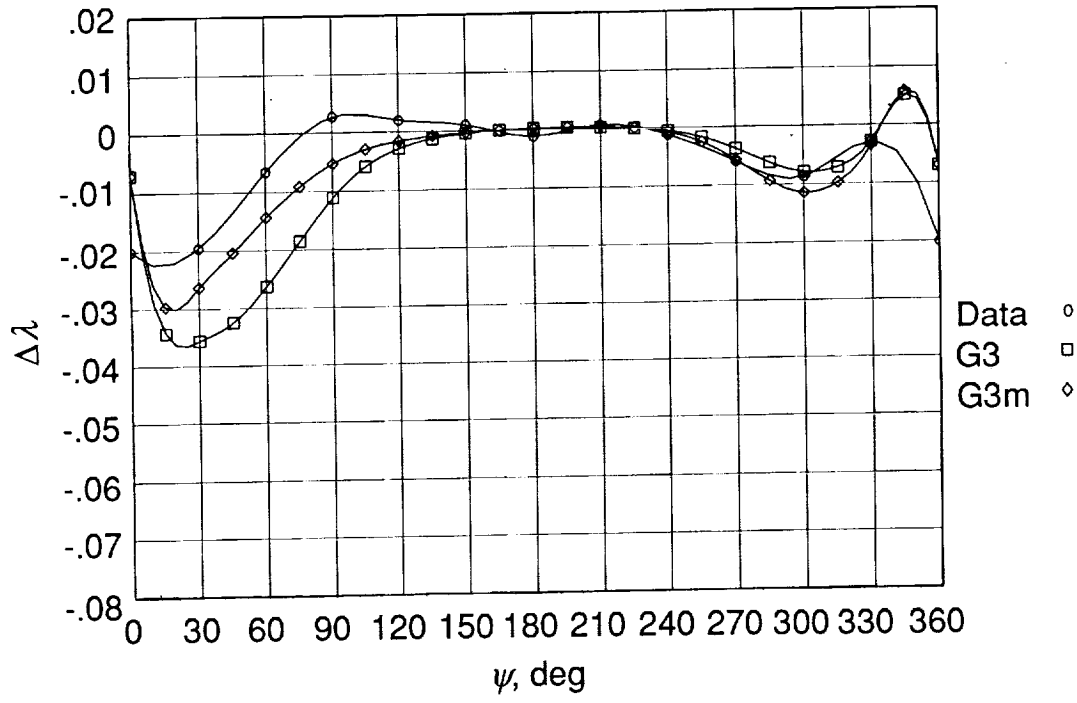

(b) $\rho = 0.79$.

Figure 13. Correlation of DOWN prediction of $\Delta\lambda$ with data of reference 29 by using the quartic circulation distribution with and without azimuthal variation of circulation. $\mu = 0.350$; $C_T = 0.0064$; $y = 0.077$.

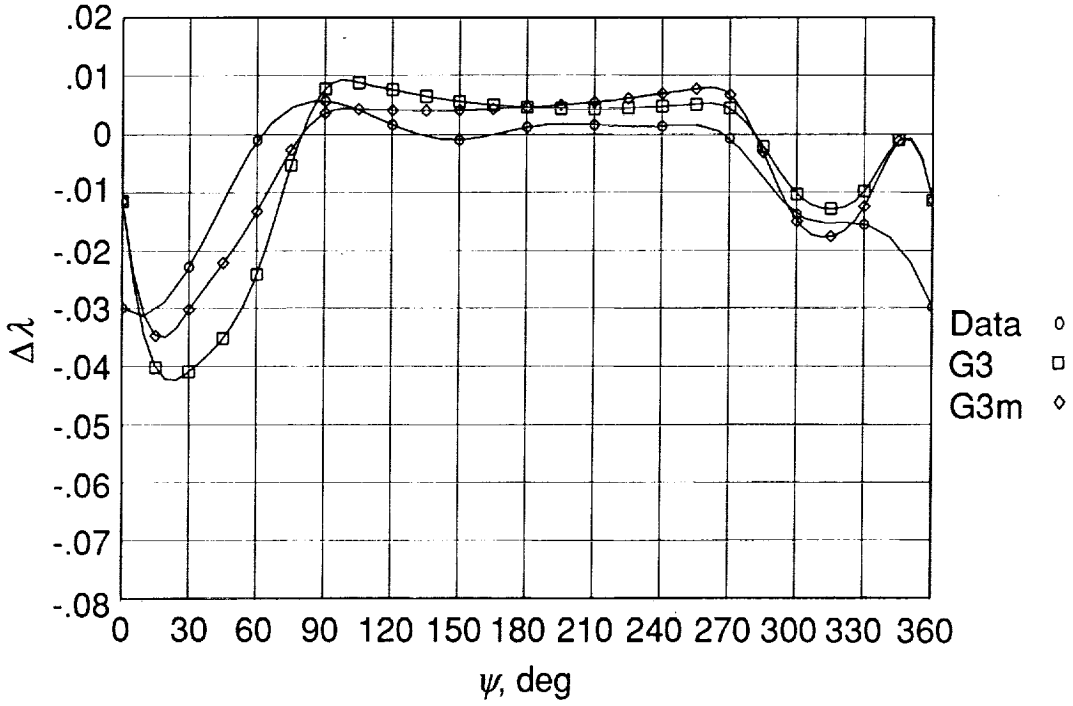

(c) $\rho = 0.98$.

Figure 13. Concluded.

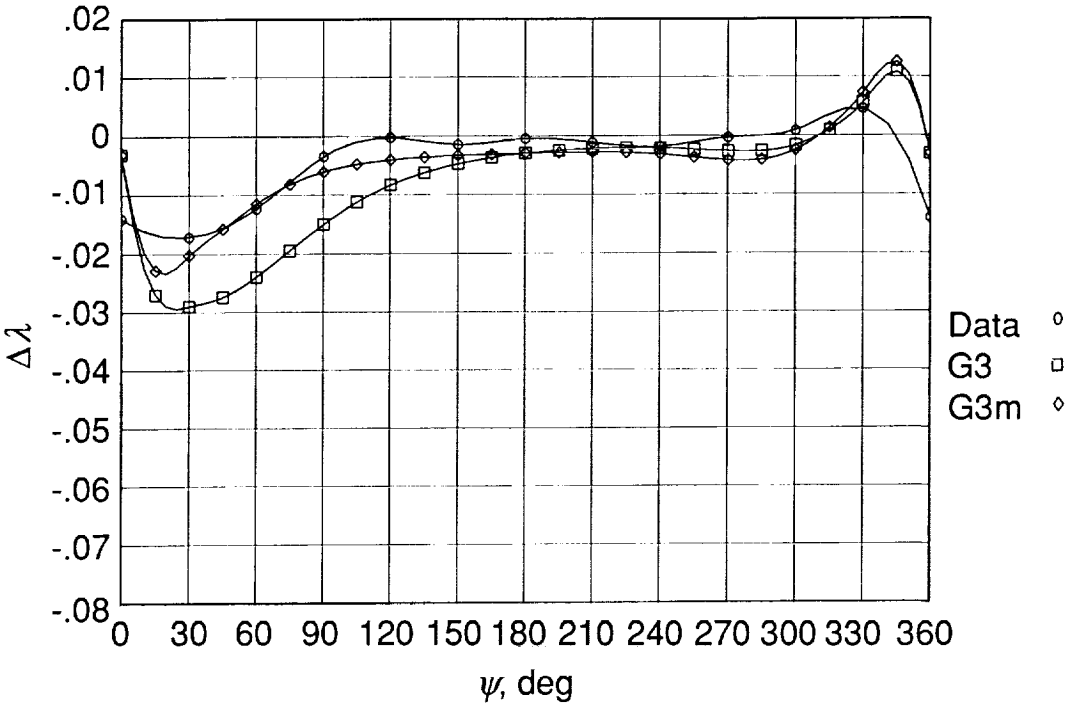

(a) $\rho = 0.60$.

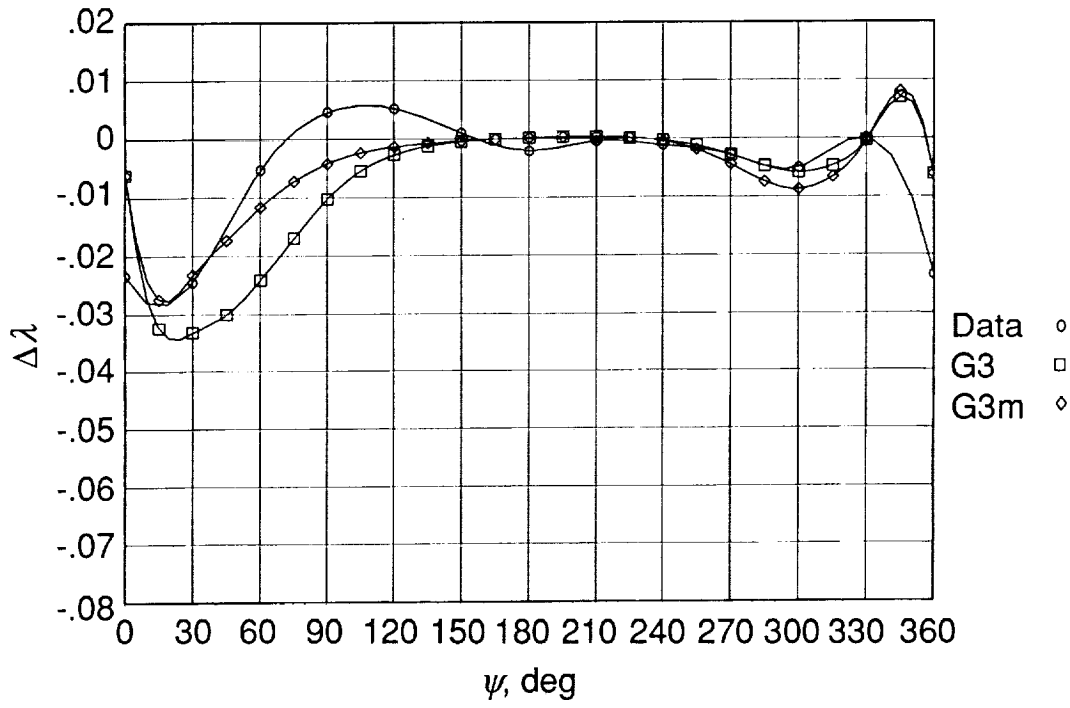

(b) $\rho = 0.79$.

Figure 14. Correlation of DOWN prediction of $\Delta\lambda$ with data of reference 30 by using the quartic circulation distribution with and without azimuthal variation of circulation. $\mu = 0.400$; $C_T = 0.0064$; $y = 0.077$.

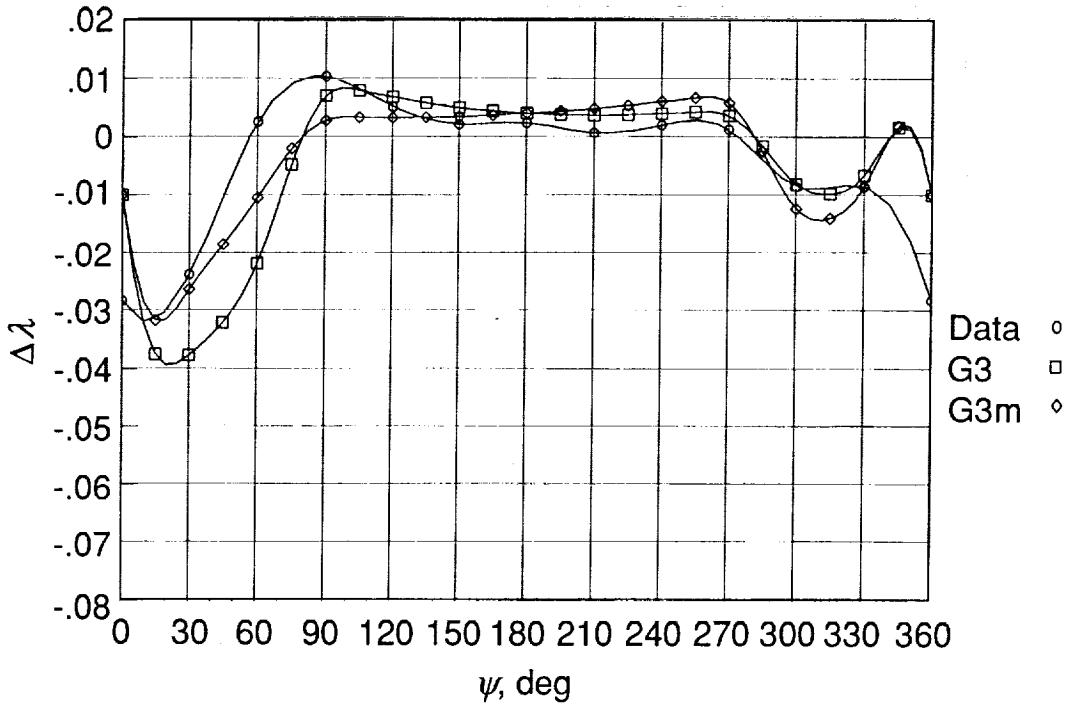

(c) $\rho = 0.98$.

Figure 14. Concluded.

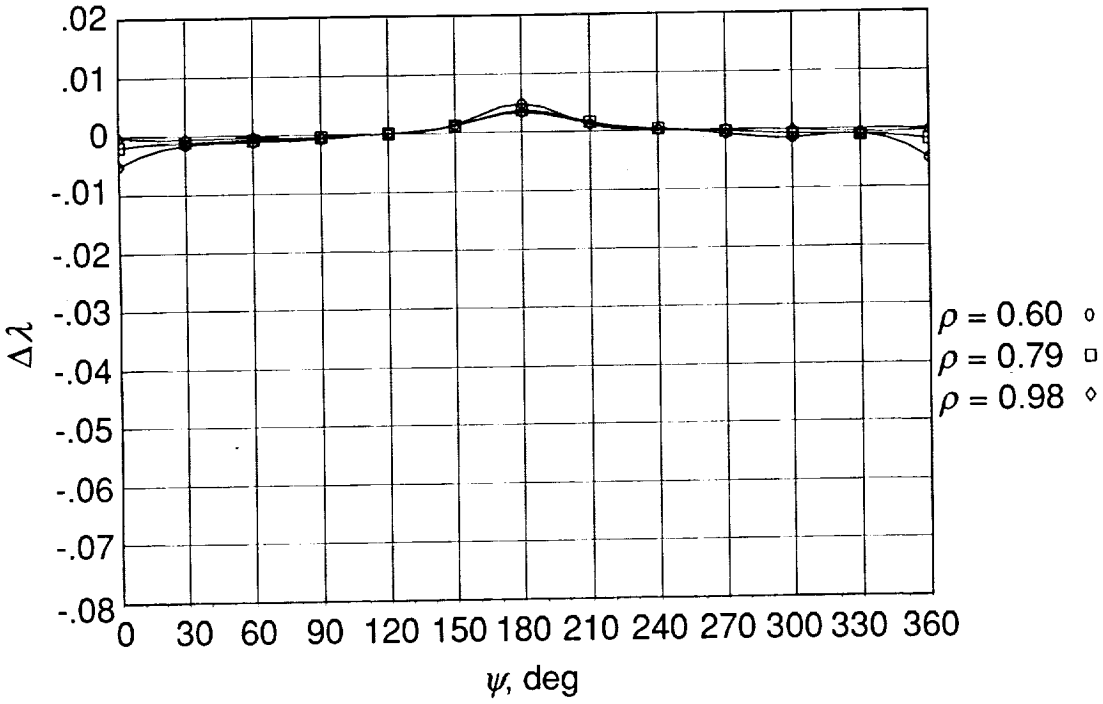

(a) $\mu = 0.15$.

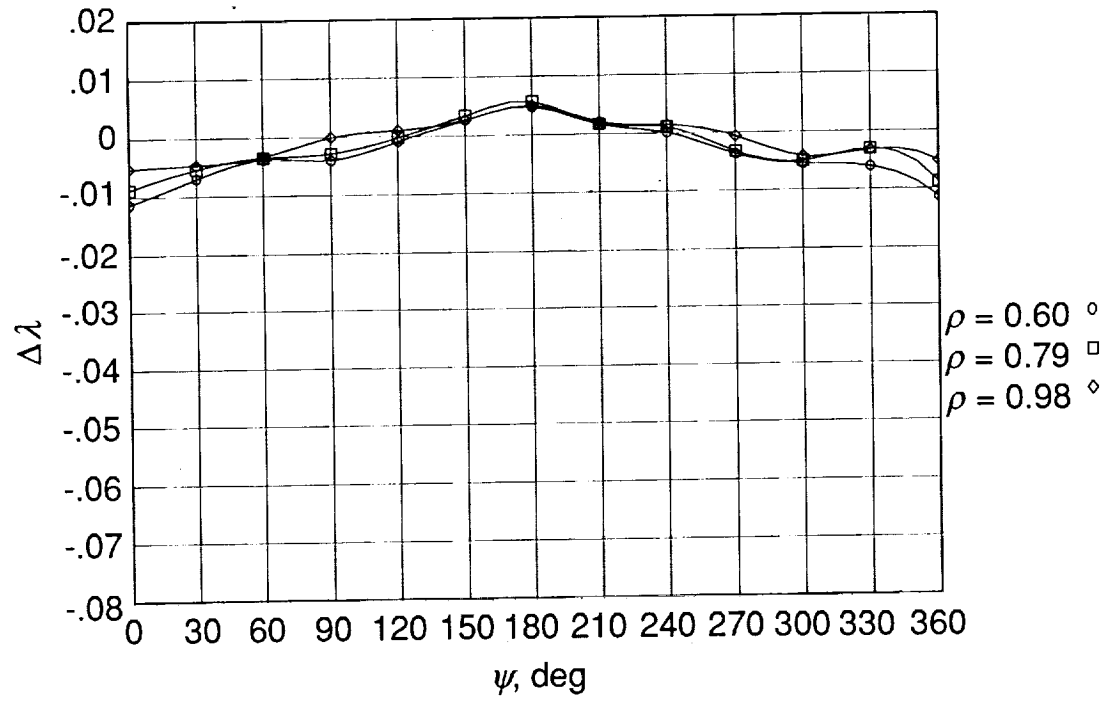

(b) $\mu = 0.23$.

Figure 15. Predicted fuselage-corrected $\Delta\lambda$ using data of references 24, 25, and 26.

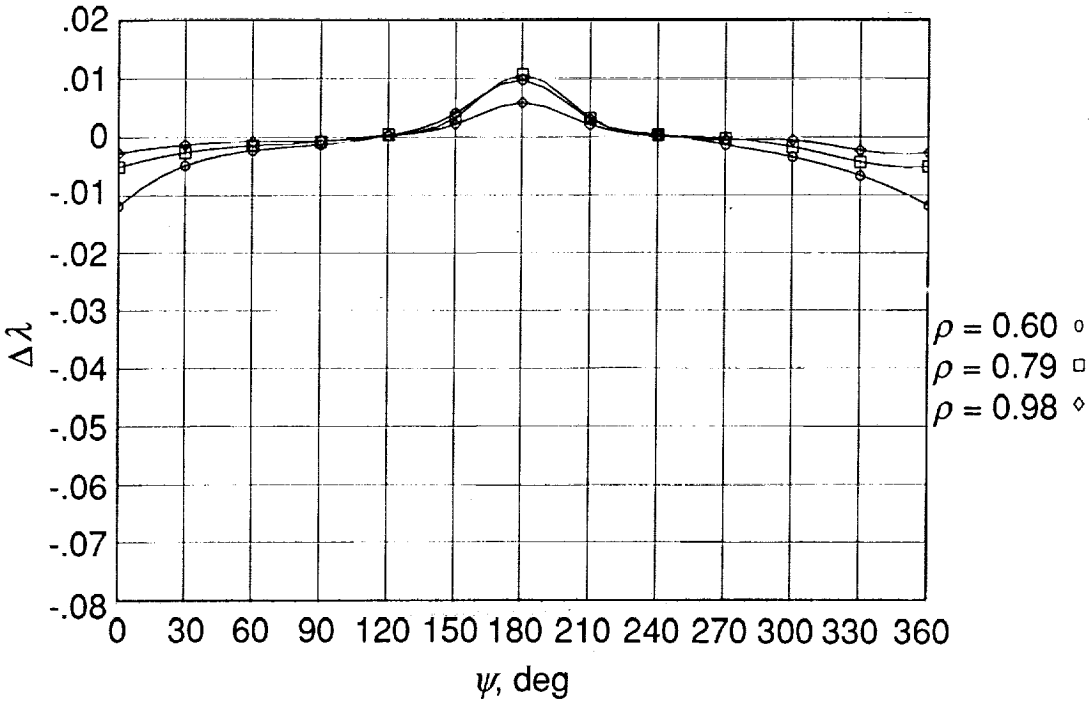

(c) $\mu = 0.30$.

Figure 15. Concluded.

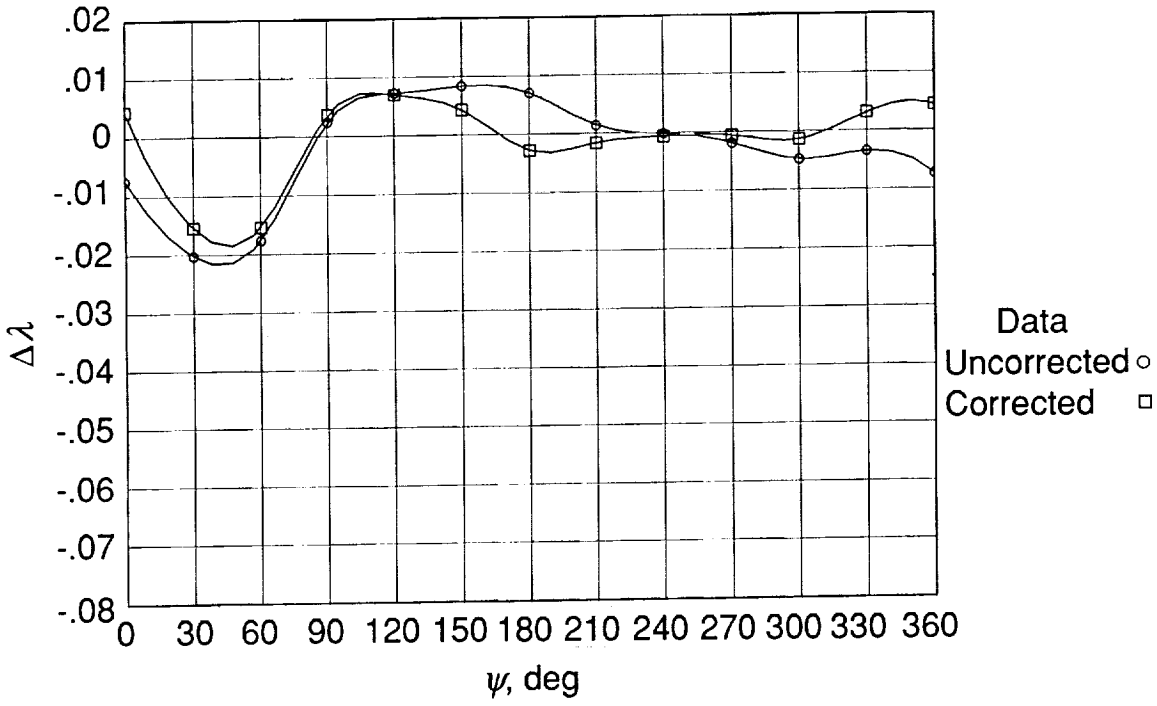

(a) $\rho = 0.60$.

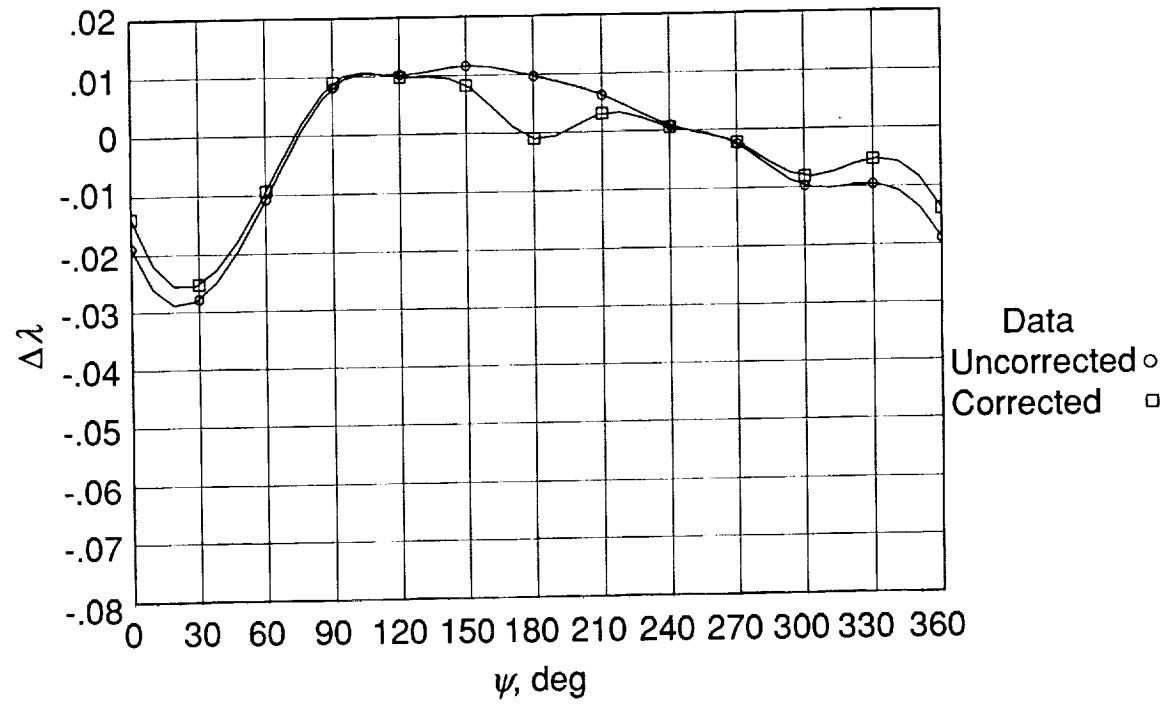

(b) $\rho = 0.79$.

Figure 16. Effect of applying a correction for the presence of the fuselage to $\Delta\lambda$ data of reference 25.

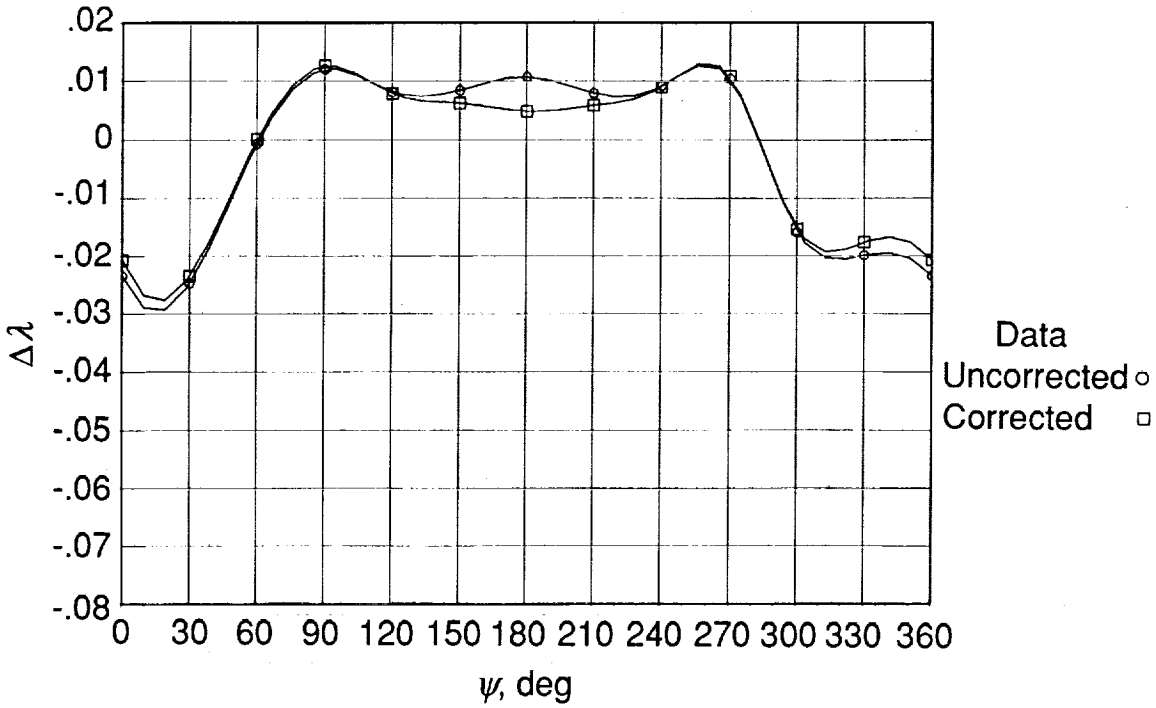

(c) $\rho = 0.98$.

Figure 16. Concluded.

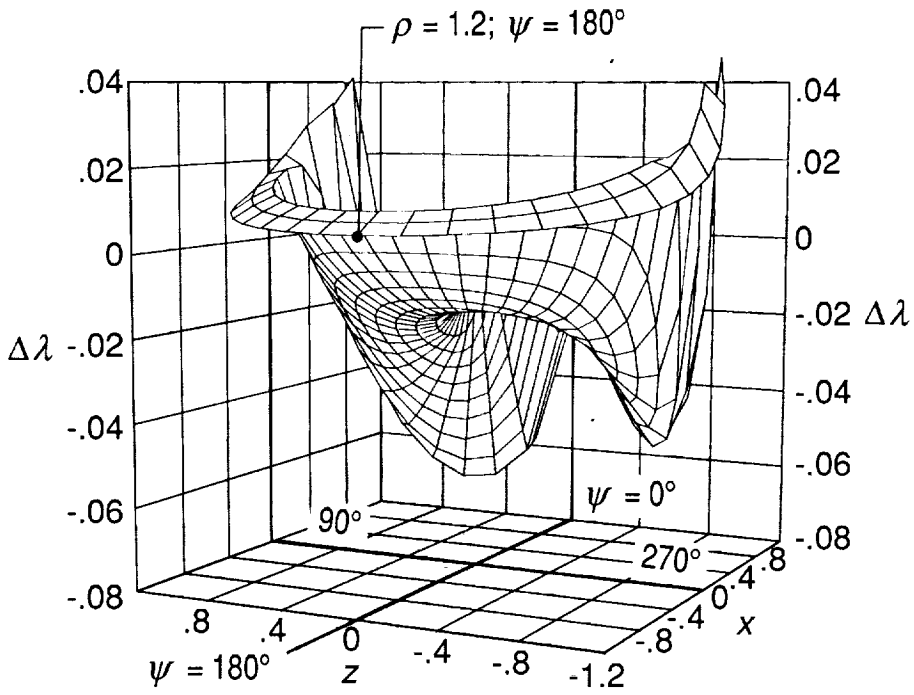

(a) DOWN prediction with G3m.

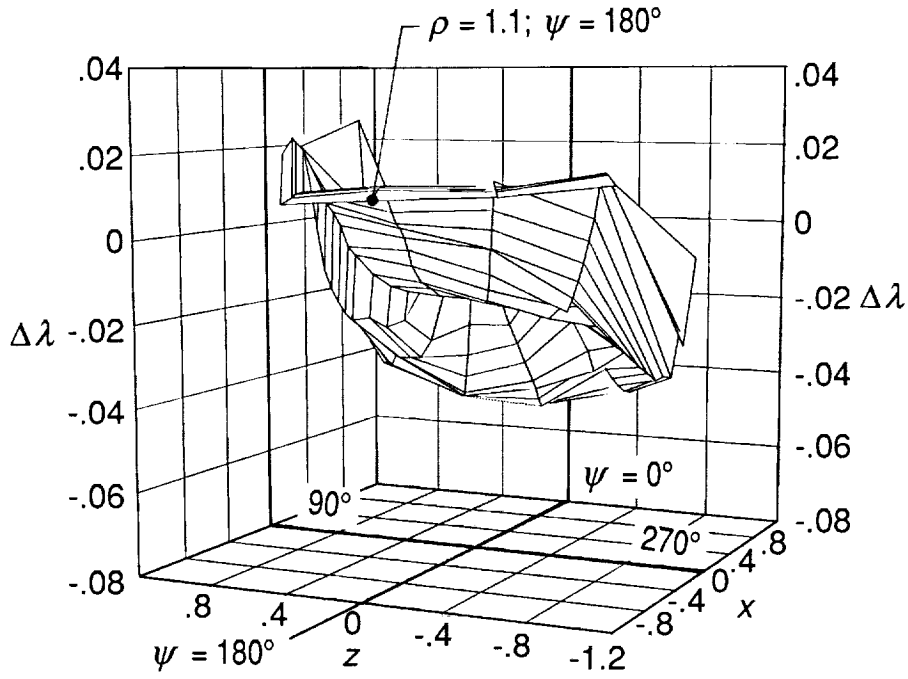

(b) Data from reference 24.

Figure 17. Comparison of DOWN prediction of $\Delta\lambda$ with data from reference 24 with $\mu = 0.149$.

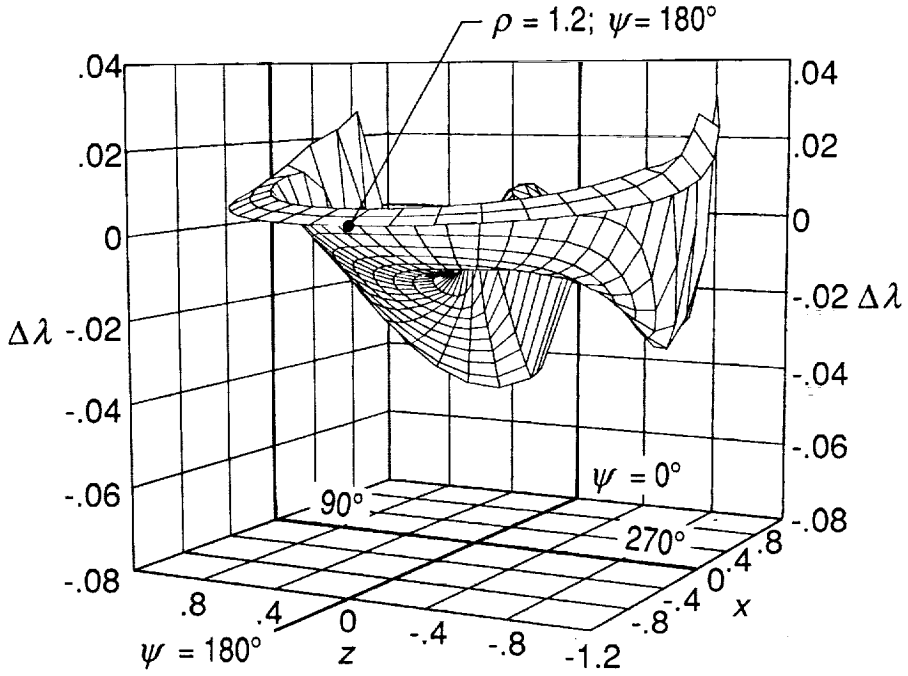

(a) DOWN prediction with G3m.

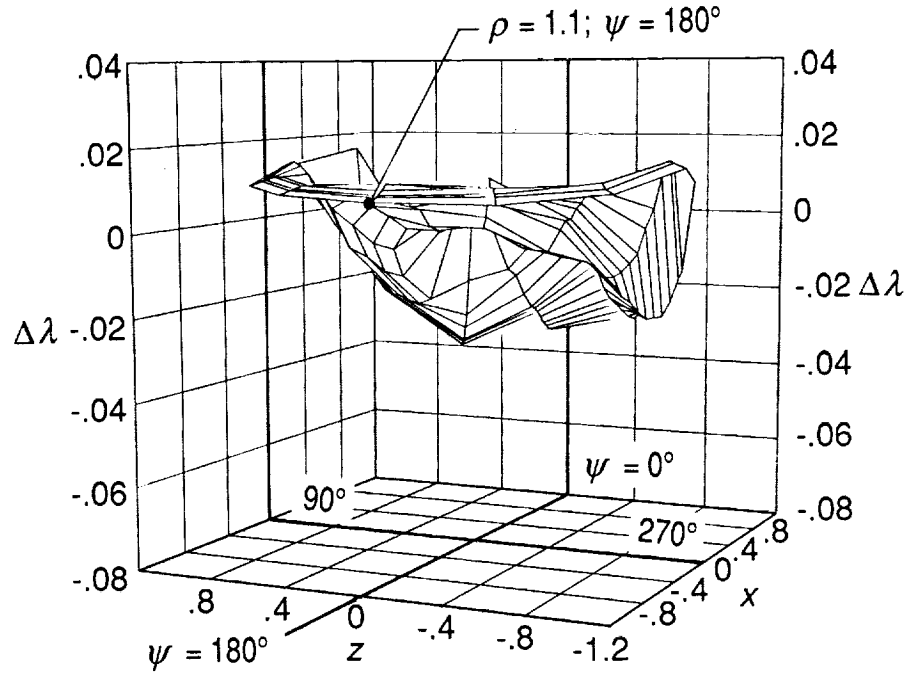

(b) Data from reference 25.

Figure 18. Comparison of DOWN prediction of $\Delta\lambda$ with data from reference 25 with $\mu = 0.230$.

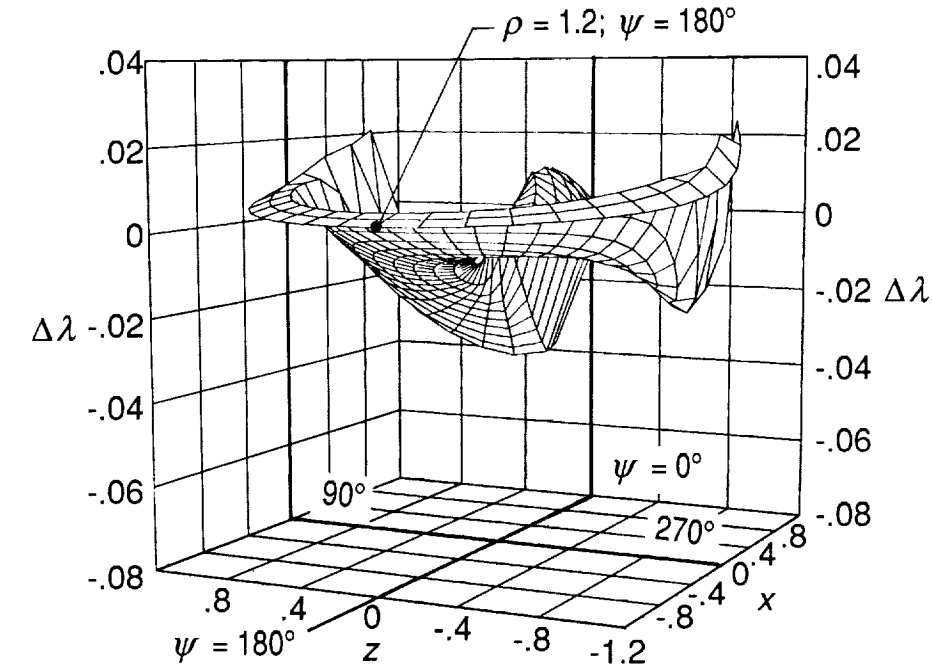

(a) DOWN prediction with G3m.

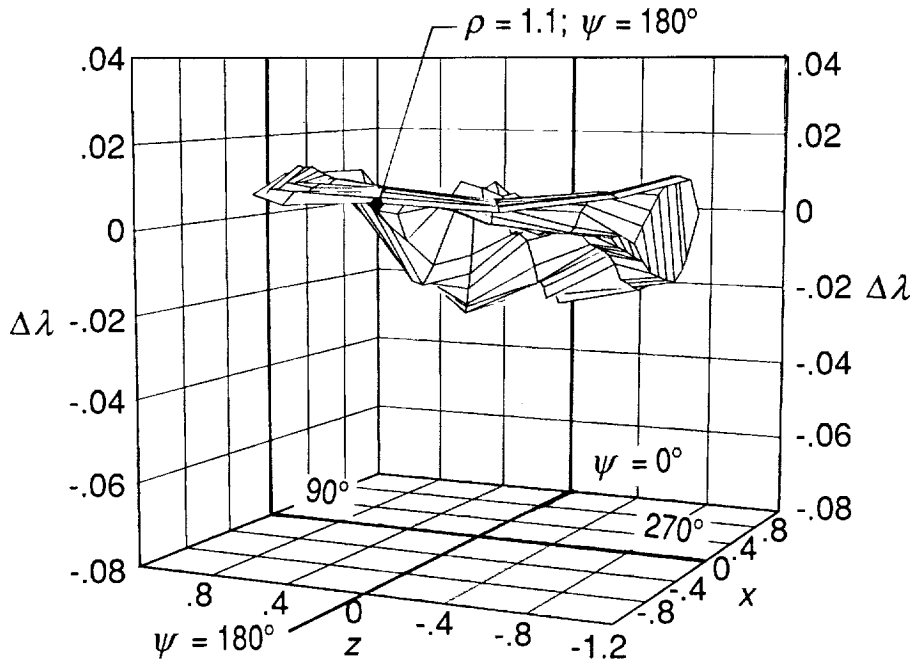

(b) Data from reference 26.

Figure 19. Comparison of DOWN prediction of $\Delta\lambda$ with data from reference 26 with $\mu = 0.300$.

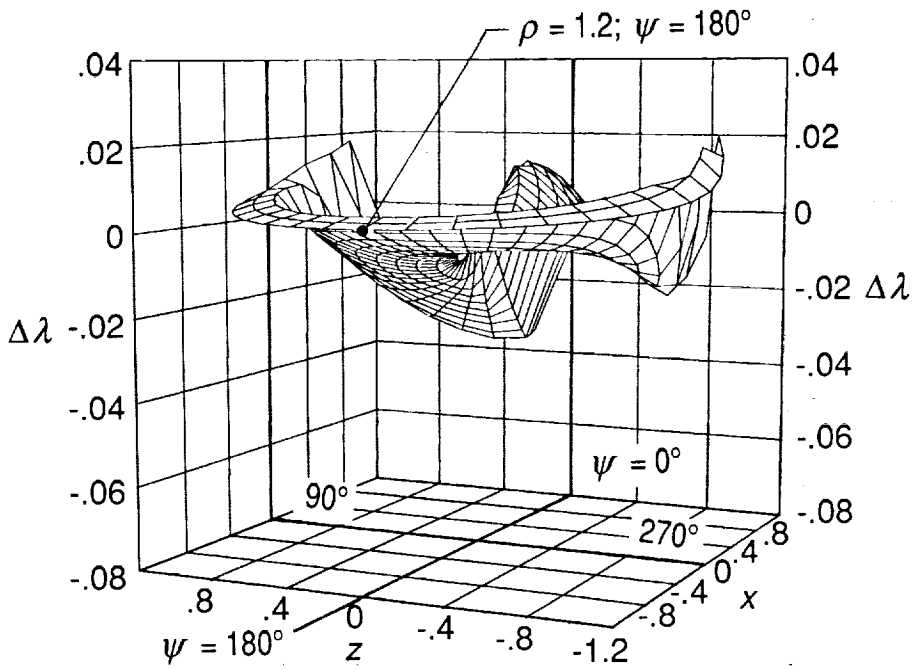

(a) DOWN prediction with G3m.

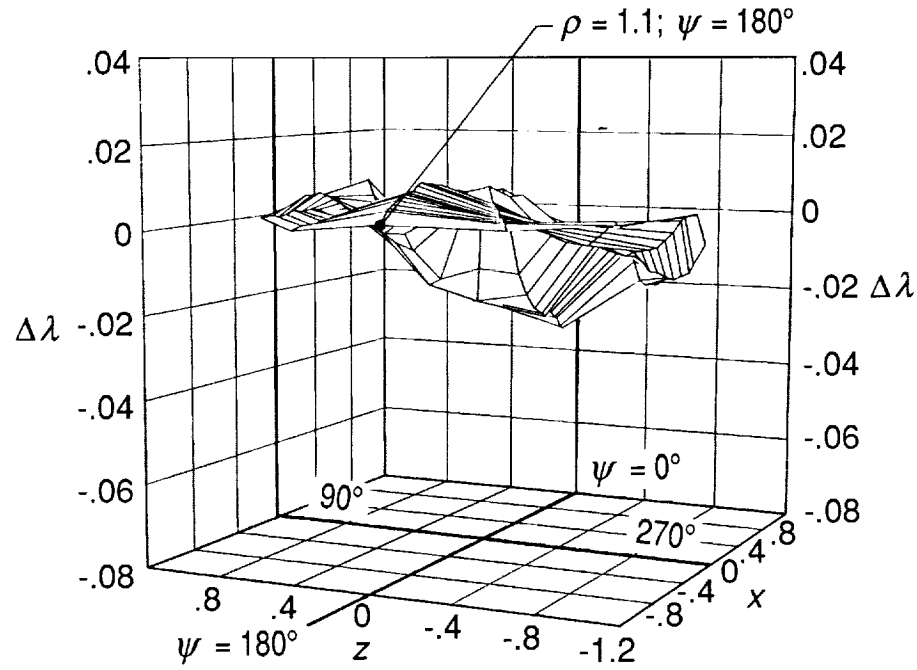

(b) Data from reference 29.

Figure 20. Comparison of DOWN prediction of $\Delta\lambda$ with data from reference 29 with $\mu = 0.350$.

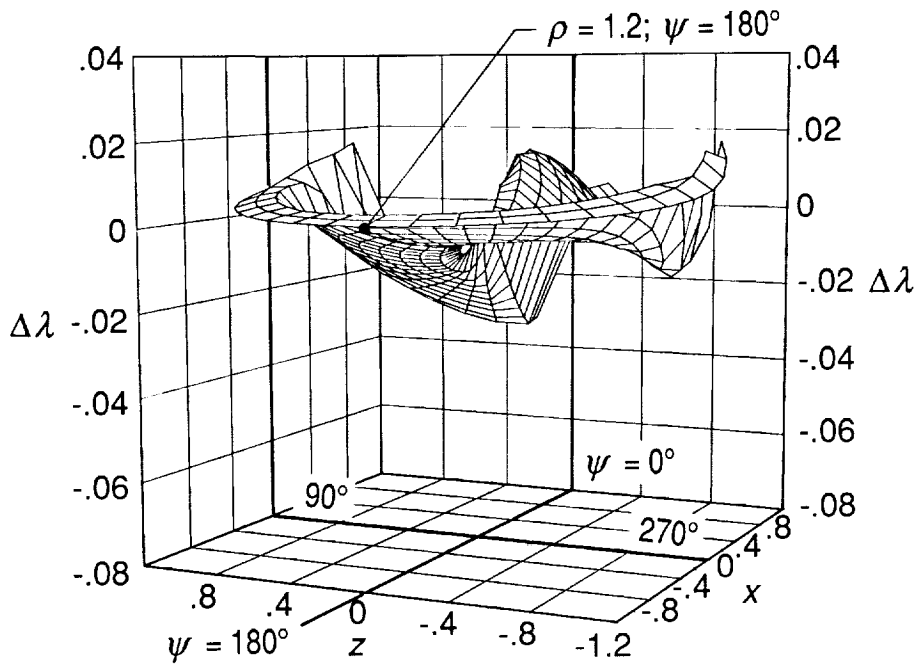

(a) DOWN prediction with G3m.

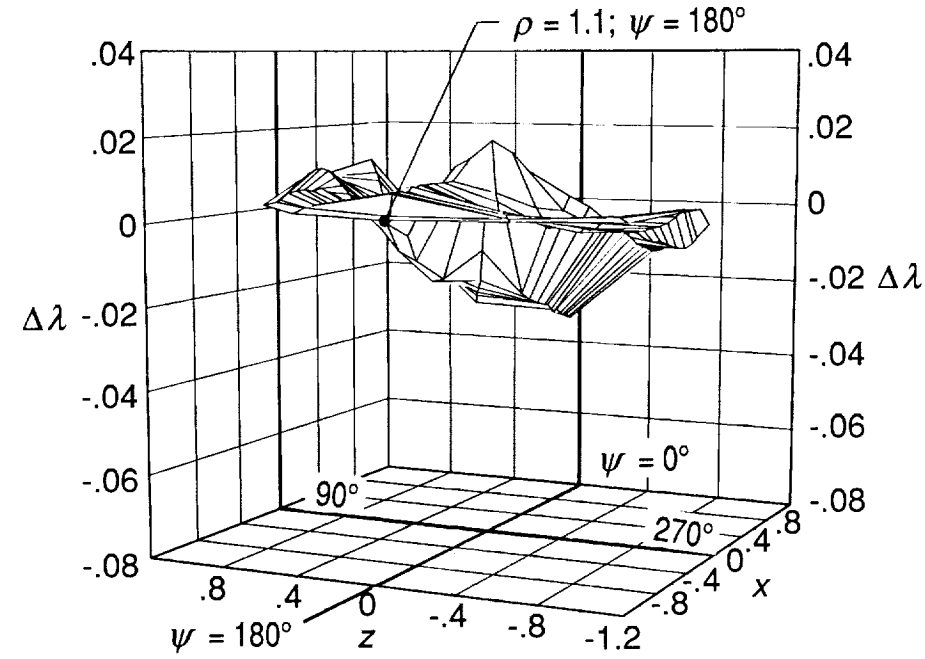

(b) Data from reference 30.

Figure 21. Comparison of DOWN prediction of $\Delta\lambda$ with data from reference 30 with $\mu = 0.400$.

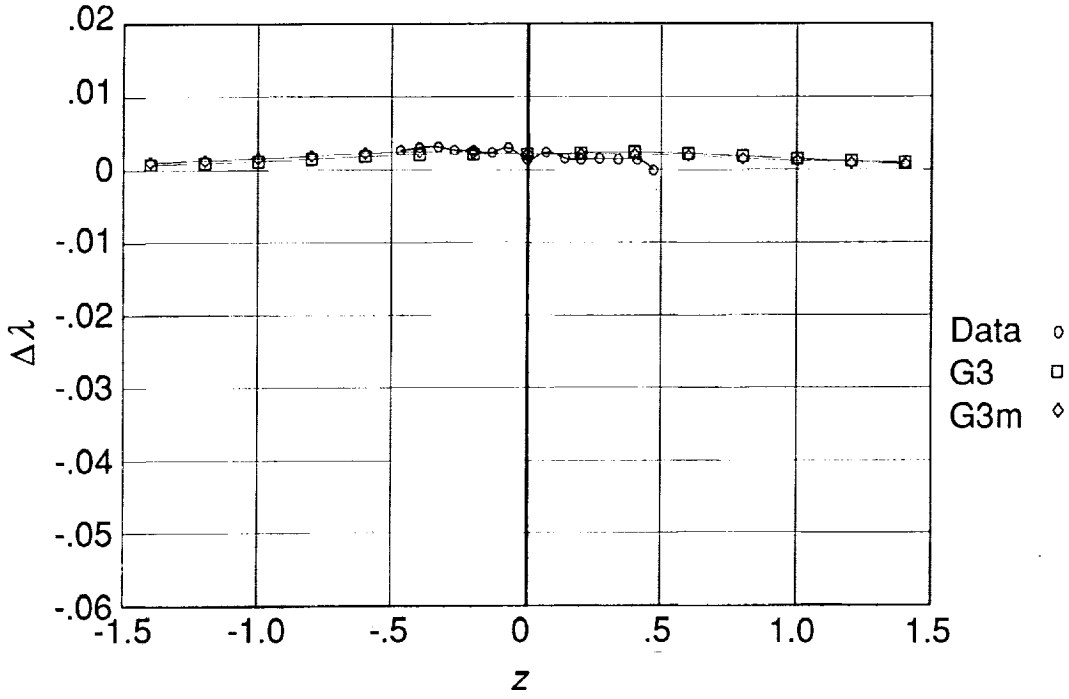

(a) $x = 1.0$ ($y = 0.16$).

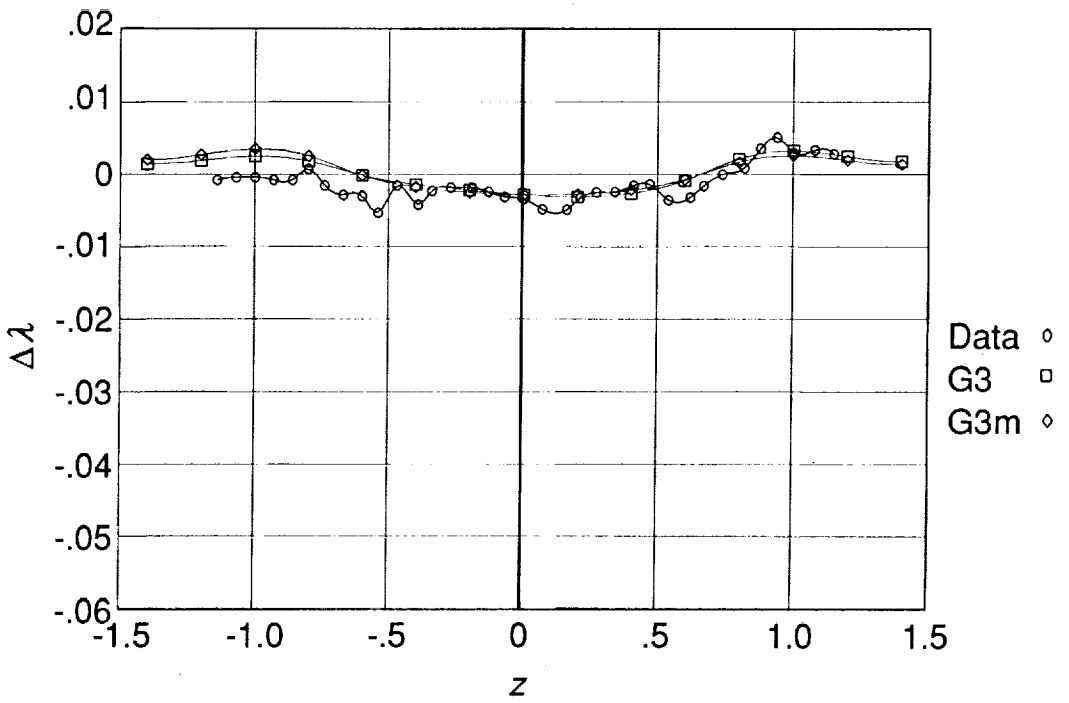

(b) $x = 0.5$ ($y = 0.17$).

Figure 22. Correlation of DOWN prediction (using quartic circulation distribution with and without azimuthal variation of circulation) of $\Delta\lambda$ with data from reference 5 for several longitudinal stations above the rotor ($y \approx 0.18$). $\mu = 0.232$; $C_T = 0.00321$.

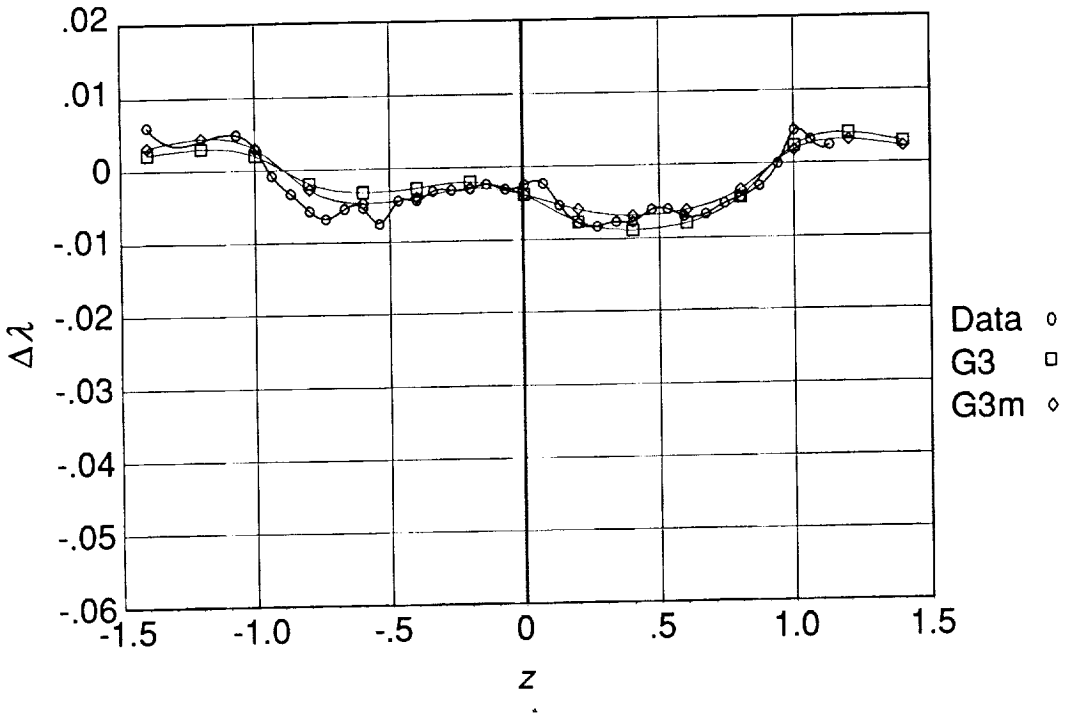

(c) $x = 0$ $(y = 0.19)$.

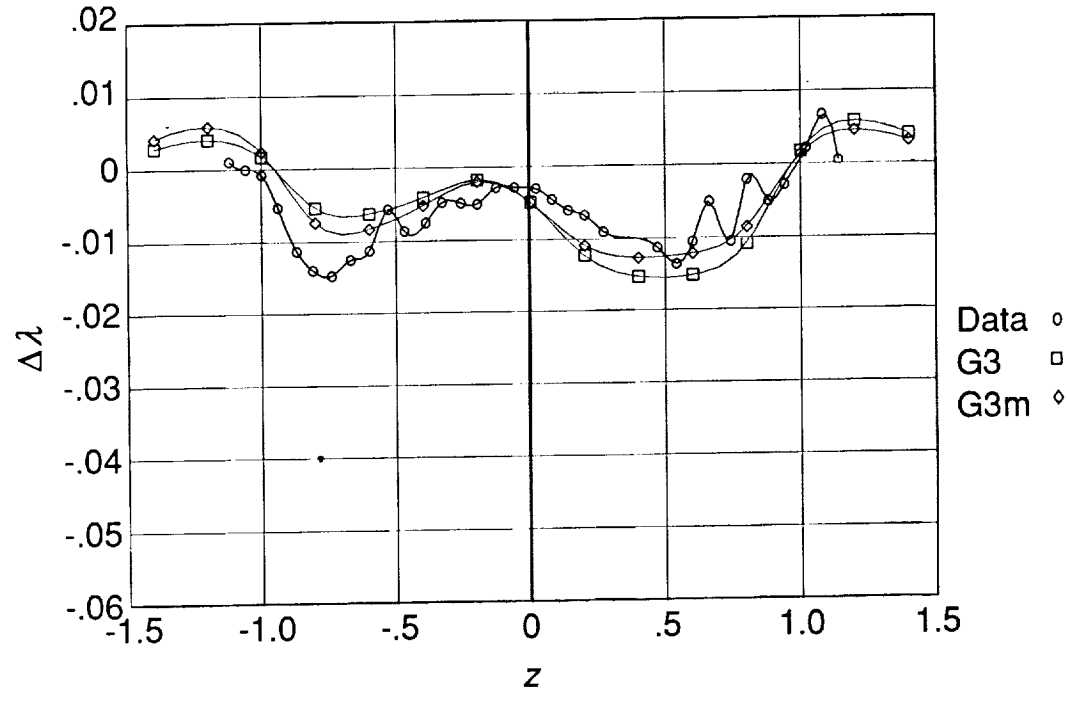

(d) $x = -0.5$ $(y = 0.19)$.

Figure 22. Continued.

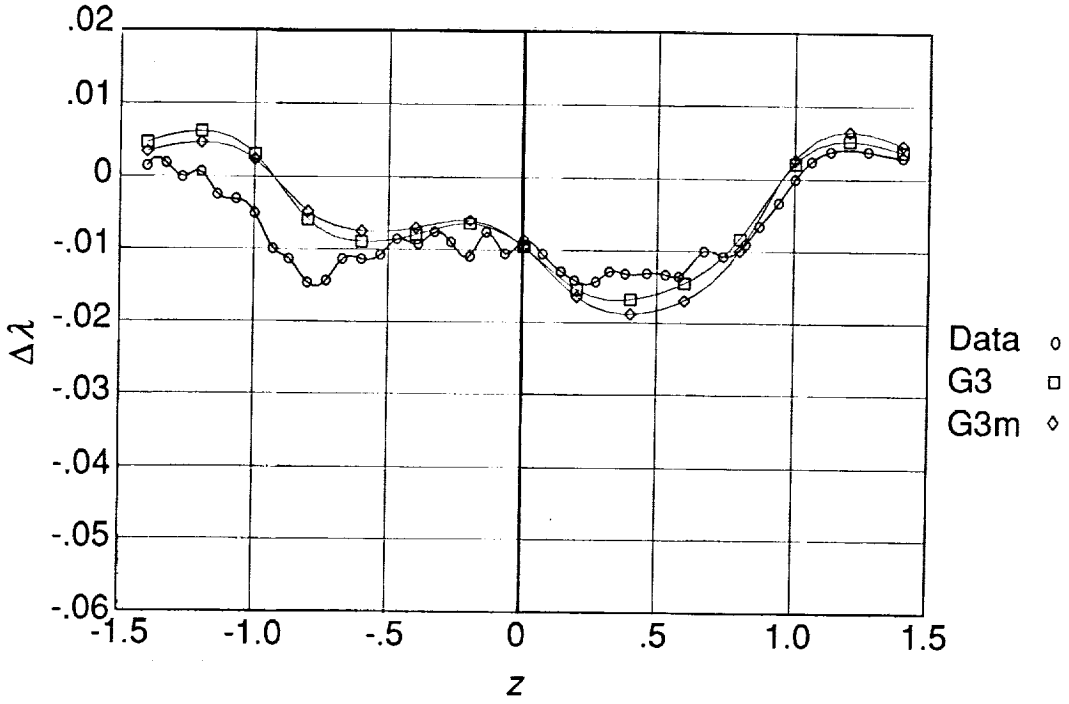

(e) $x = -1.07$ ($y = 0.19$).

Figure 22. Concluded.

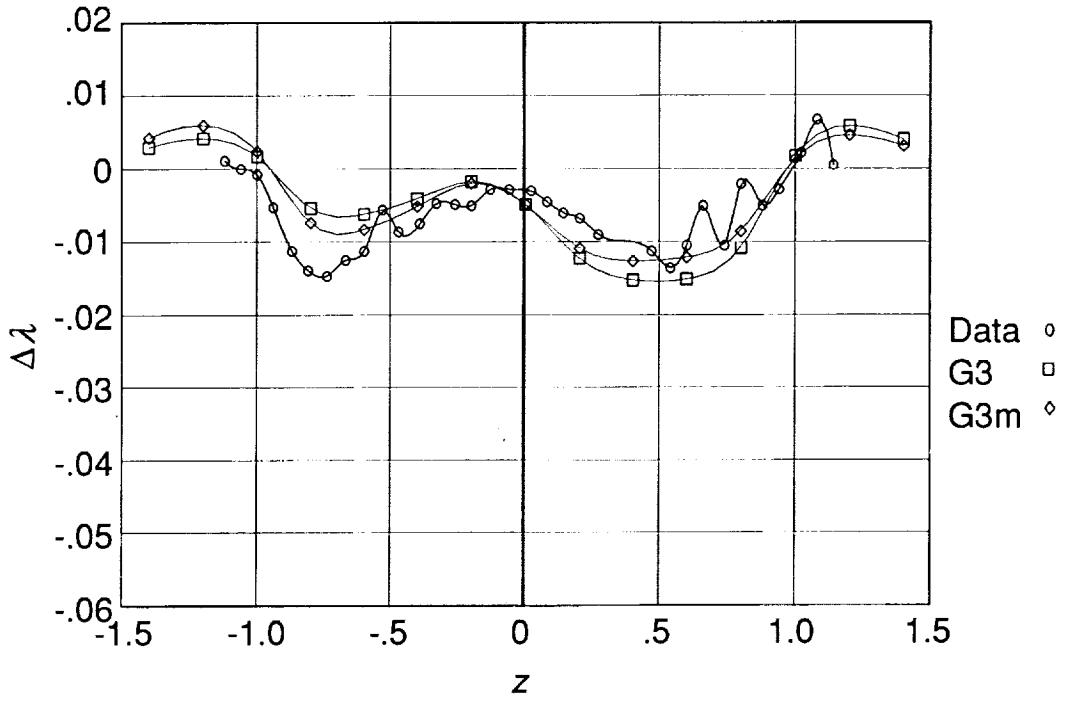

(a) $y = 0.19$.

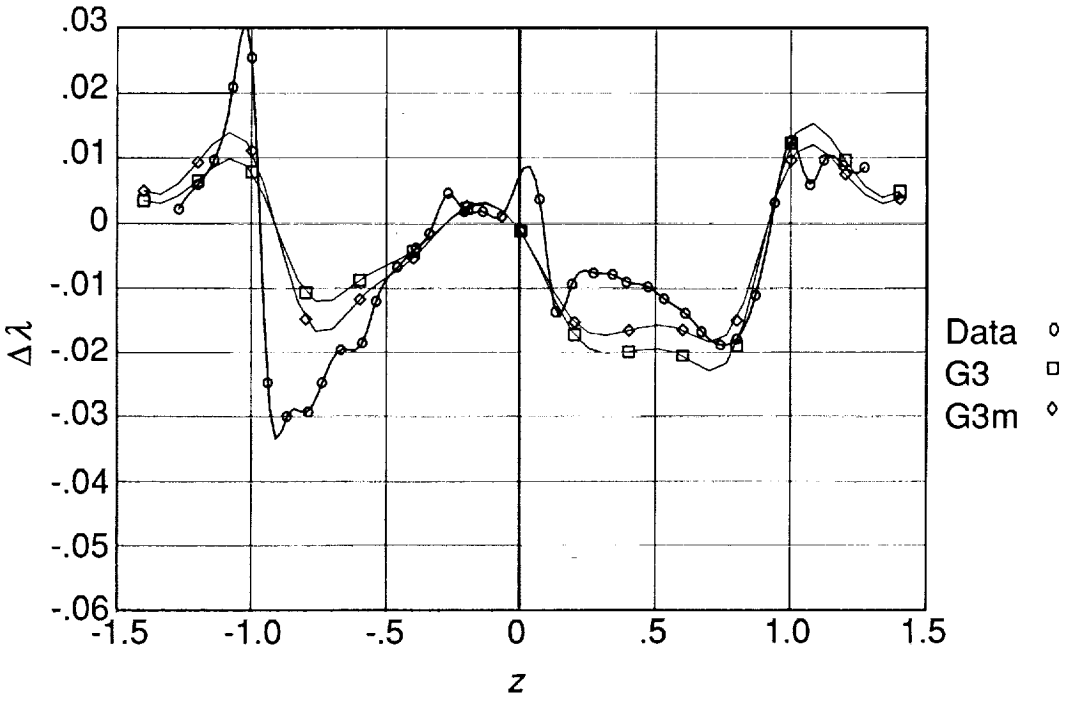

(b) $y = -0.07$.

Figure 23. Correlation of DOWN prediction (using quartic circulation distribution with and without azimuthal variation of circulation) of $\Delta\lambda$ with data from reference 5 for several vertical stations at $x = -0.50$. $\mu = 0.232$; $C_T = 0.00321$.

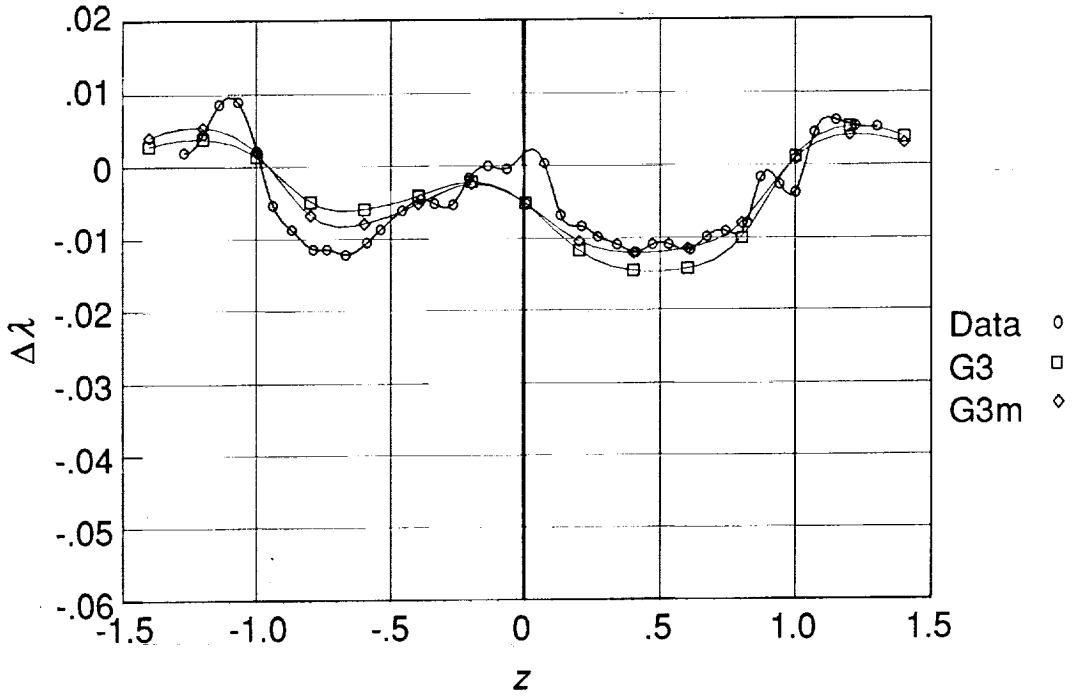

(c) $y = -0.21$.

Figure 23. Concluded.

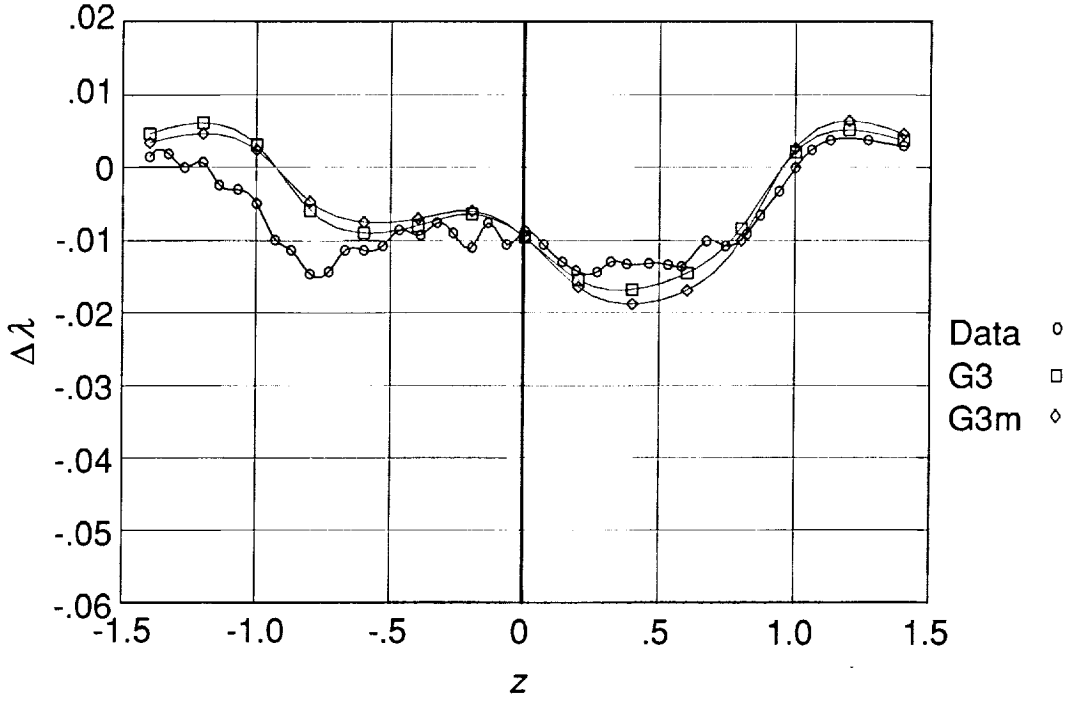

(a) $y = 0.21$.

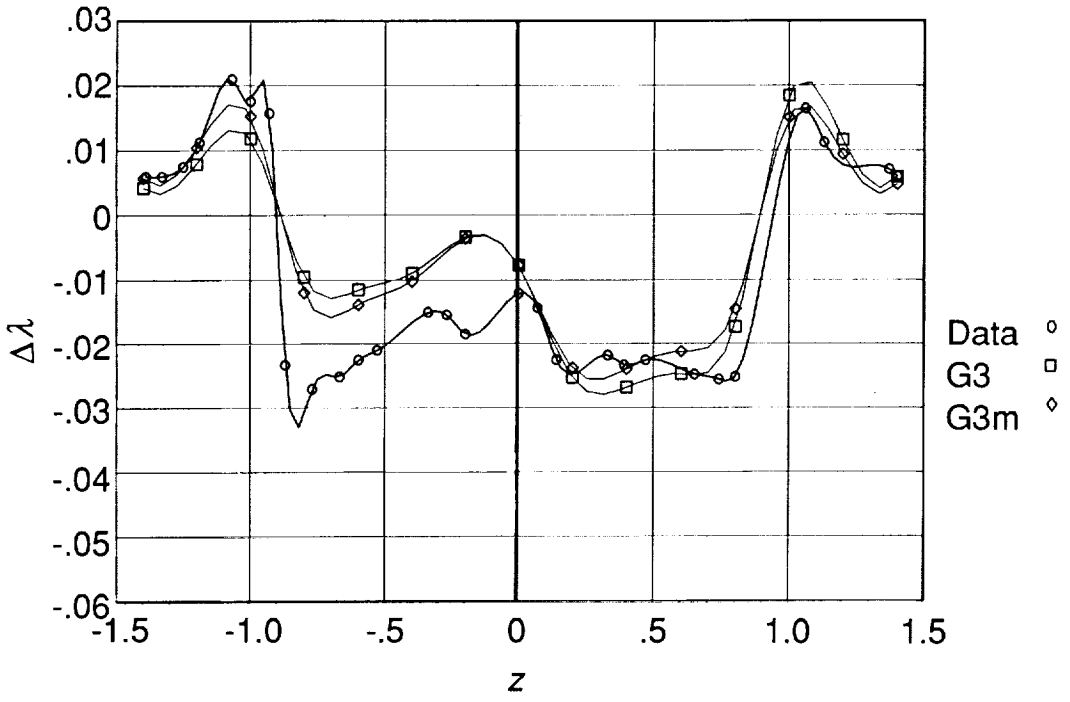

(b) $y = -0.06$.

Figure 24. Correlation of DOWN prediction (using quartic circulation distribution with and without azimuthal variation of circulation) of $\Delta\lambda$ with data from reference 5 for several vertical stations at $x = -1.07$. $\mu = 0.232$; $C_T = 0.00321$.

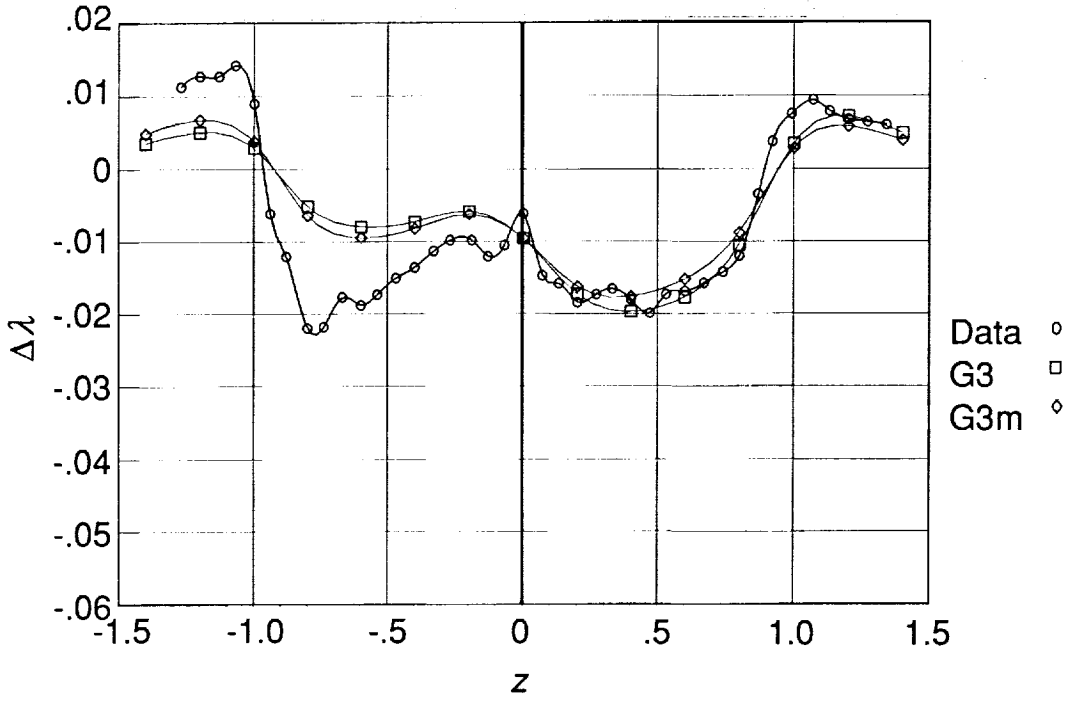

(c) $y = -0.19$.

Figure 24. Concluded.

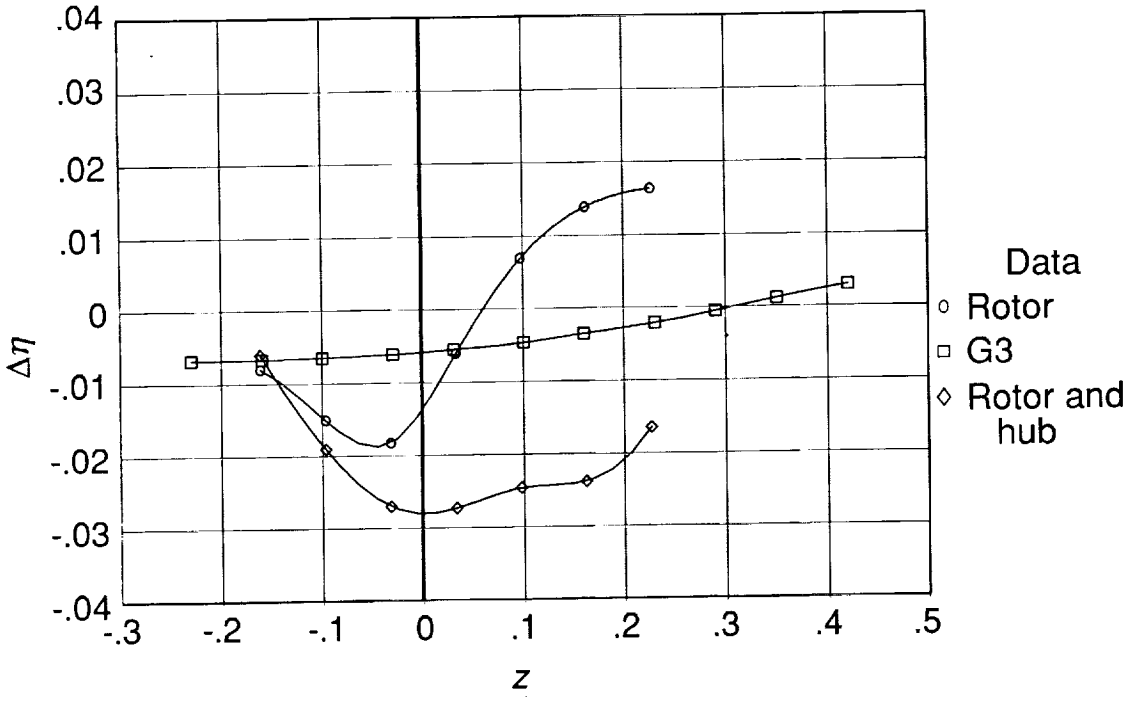

(a) $y = -0.21$.

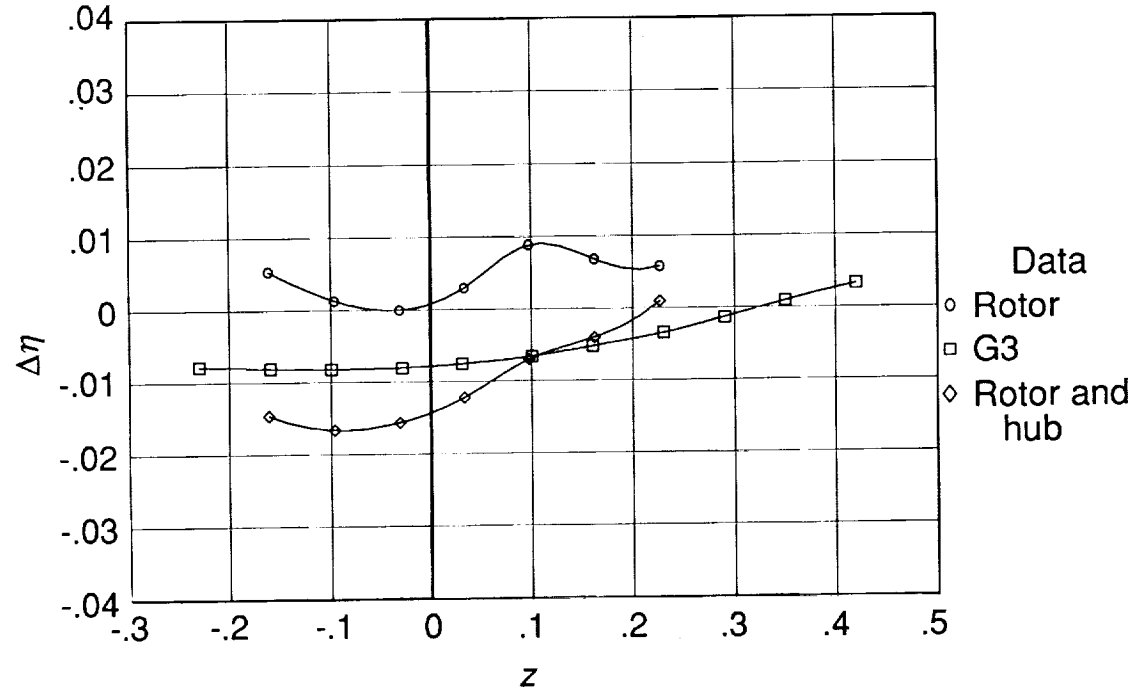

(b) $y = -0.31$.

Figure 25. Correlation of DOWN prediction (using quartic circulation distribution) of $\Delta\eta$ with data from reference 37 for several vertical stations at $x = -1.70$. $\mu = 0.29$; $C_T = 0.006$.

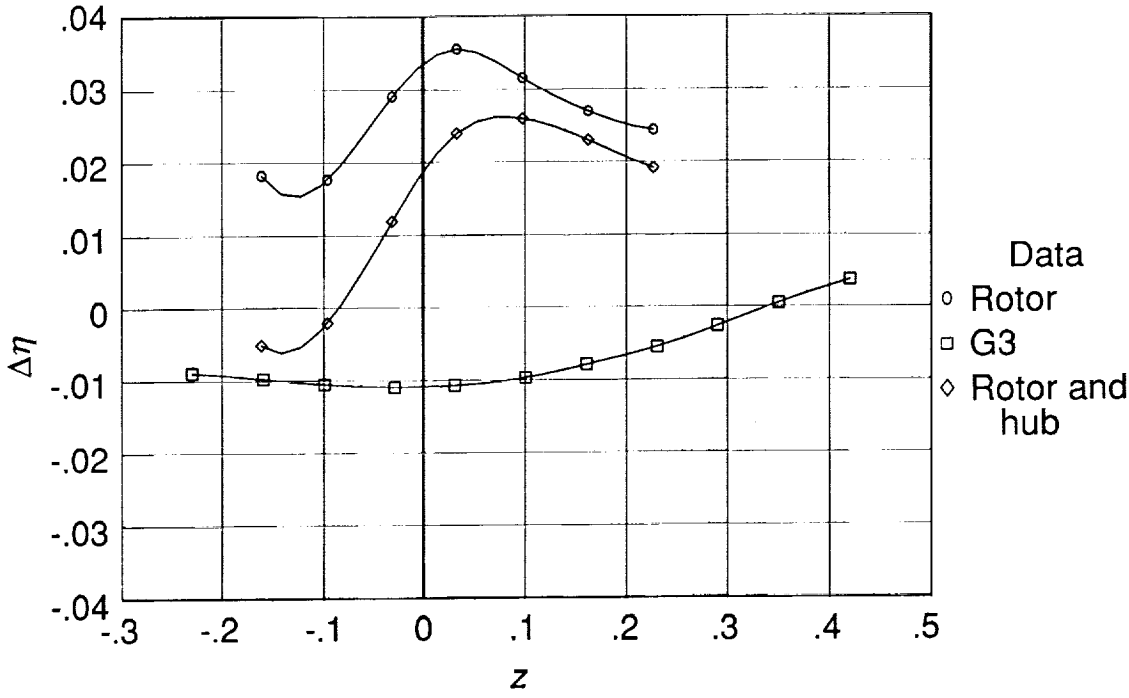

(c) $y = -0.41$.

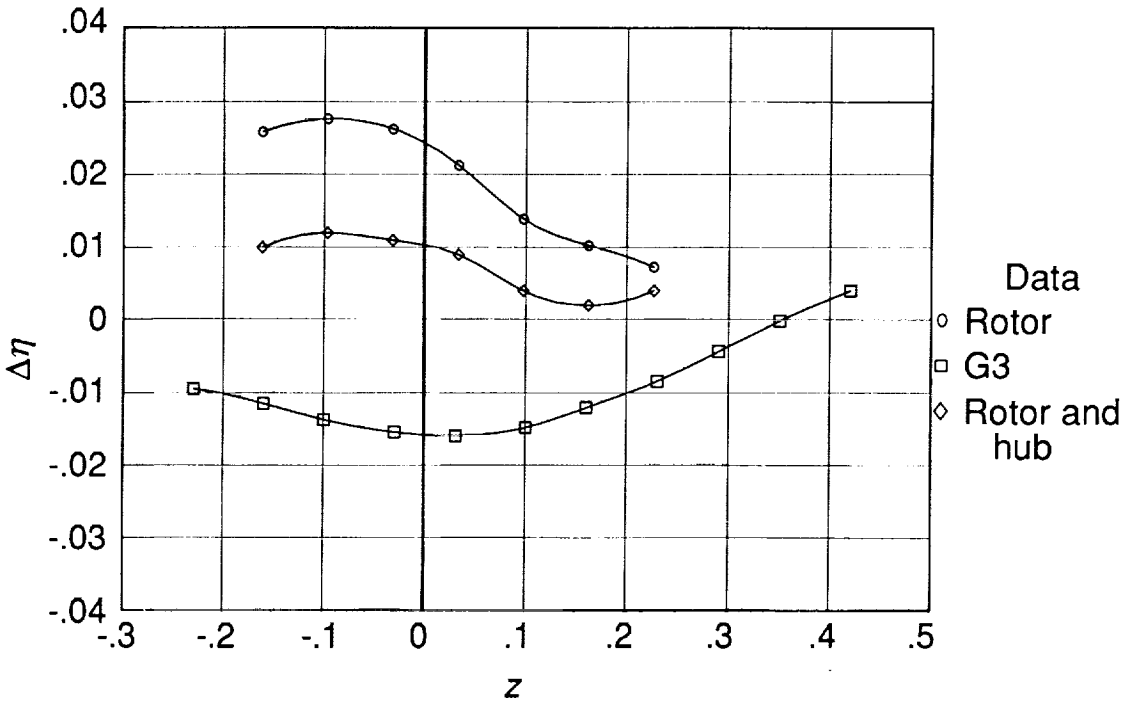

(d) $y = -0.51$.

Figure 25. Concluded.

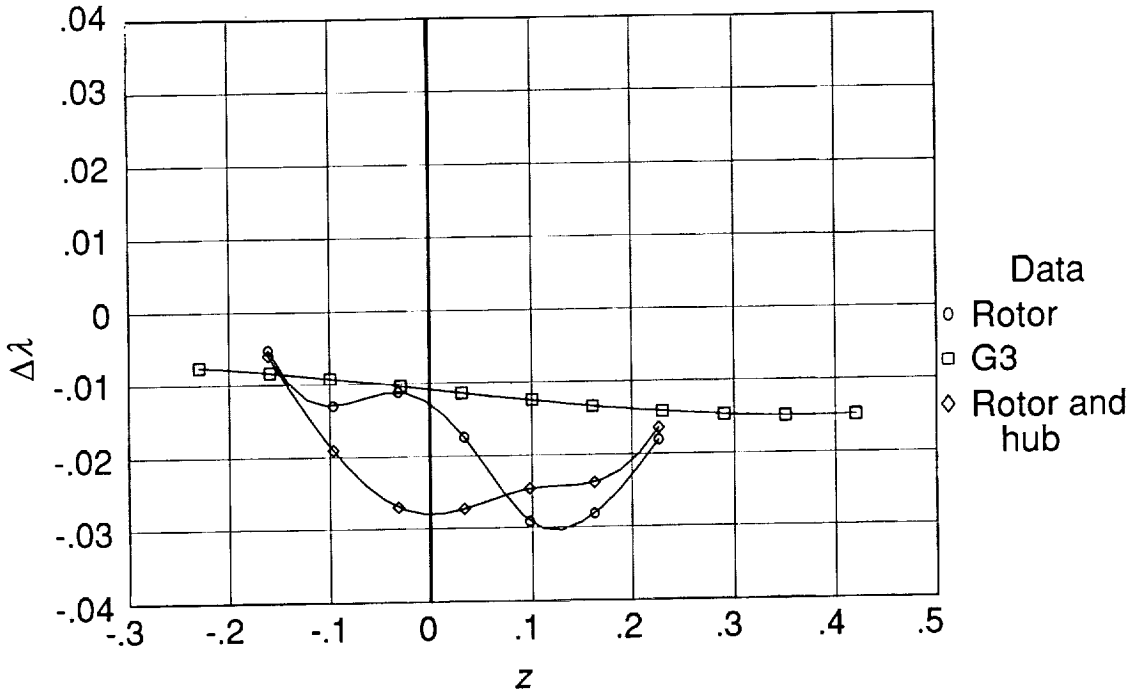

(a) $y = -0.21$.

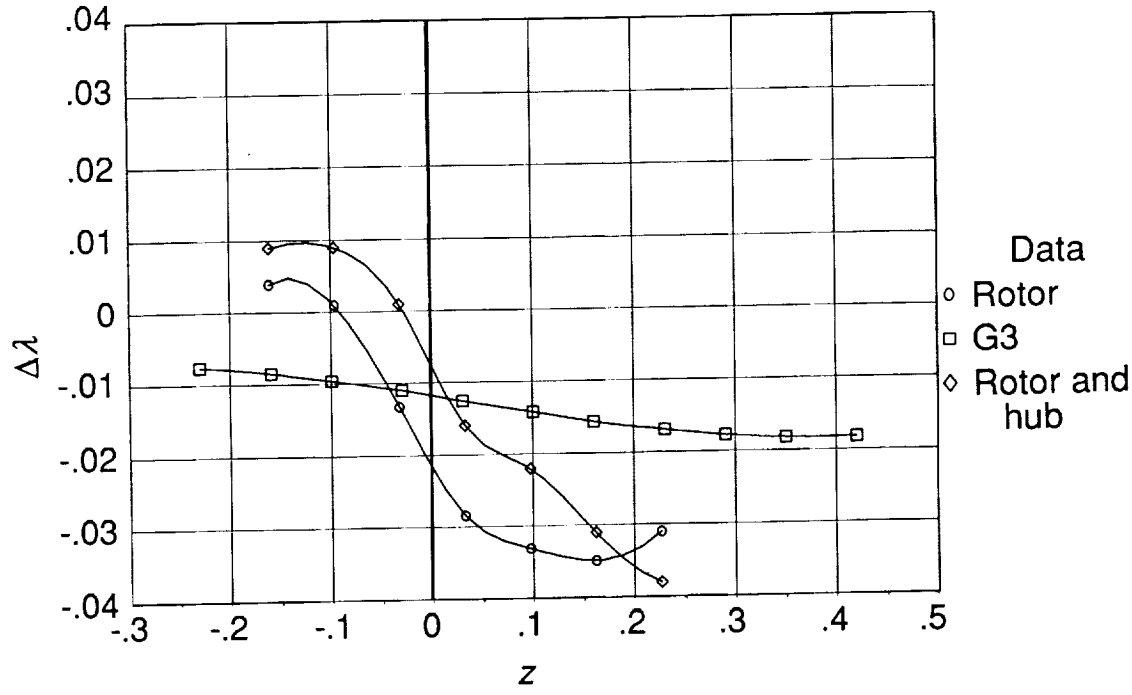

(b) $y = -0.31$.

Figure 26. Correlation of DOWN prediction (using quartic circulation) of $\Delta\lambda$ with data from reference 37 for several vertical stations at $x = -1.70$. $\mu = 0.29$; $C_T = 0.006$.

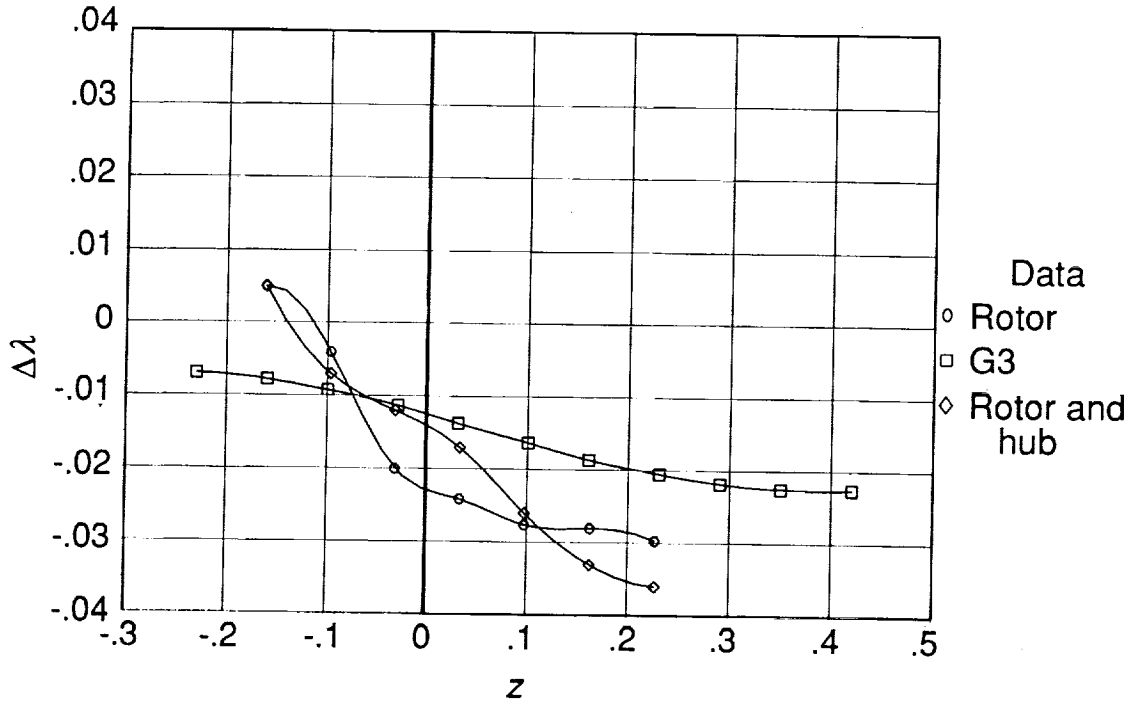

(c) $y = -0.41$.

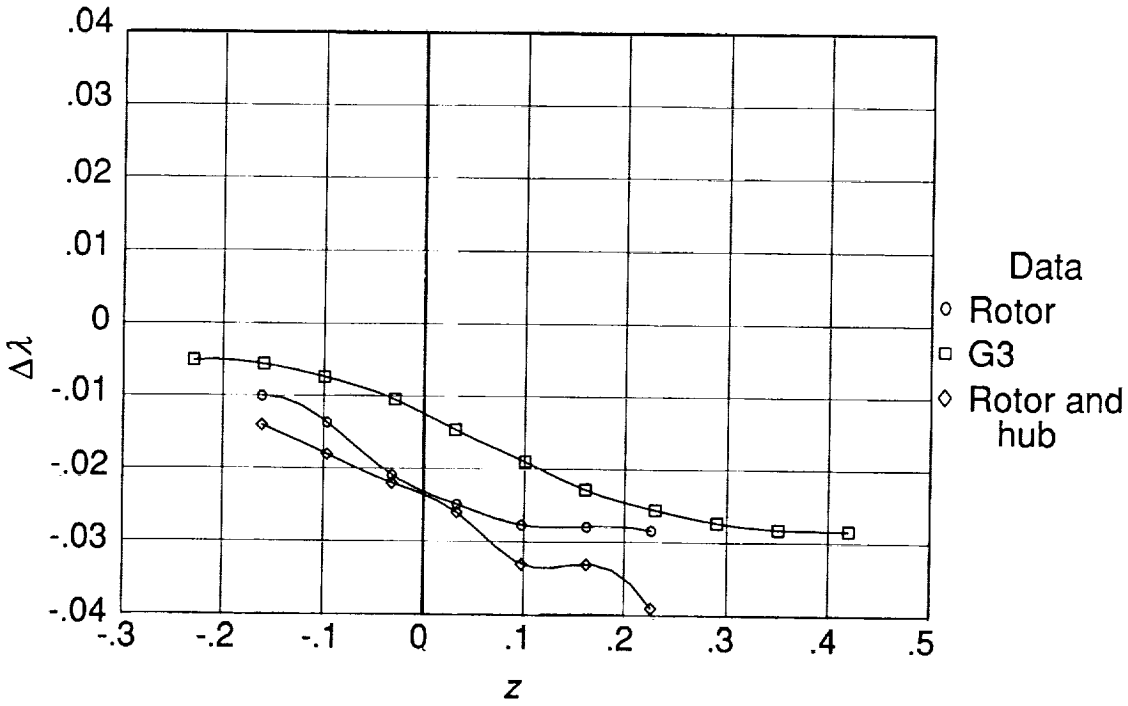

(d) $y = -0.51$.

Figure 26. Concluded.

REPORT DOCUMENTATION PAGE

Form Approved
OMB No. 0704-0188

1. AGENCY USE ONLY *(Leave blank)*	2. REPORT DATE	3. REPORT TYPE AND DATES COVERED
	April 1992	Technical Memorandum

4. TITLE AND SUBTITLE
Experimental Evaluation of a Flat Wake Theory for Predicting Rotor Inflow-Wake Velocities

5. FUNDING NUMBERS
WU 505-59-36-01
PR 1L162211A47A

6. AUTHOR(S)
John C. Wilson

7. PERFORMING ORGANIZATION NAME(S) AND ADDRESS(ES)
Aeroflightdynamics Directorate AVSCOM
JRPO Langley
Langley Research Center
Hampton, VA 23665-5225

8. PERFORMING ORGANIZATION REPORT NUMBER
L-16953

9. SPONSORING/MONITORING AGENCY NAME(S) AND ADDRESS(ES)
National Aeronautics and Space Administration
Washington, DC 20546-0001
and
U.S. Army Aviation Systems Command
St. Louis, MO 63120-1798

10. SPONSORING/MONITORING AGENCY REPORT NUMBER
NASA TM-4334
AVSCOM TR-92-B-004

11. SUPPLEMENTARY NOTES
Wilson: Aeroflightdynamics Directorate AVSCOM, JRPO—Langley, Hampton, VA.

12a. DISTRIBUTION/AVAILABILITY STATEMENT
Unclassified Unlimited

Subject Category 02

12b. DISTRIBUTION CODE

13. ABSTRACT *(Maximum 200 words)*

The theory for predicting helicopter inflow-wake velocities called *flat wake theory* was correlated with several sets of experimental data. The theory was developed by V. E. Baskin of the USSR, and a computer code known as DOWN was developed at Princeton University to implement the theory. The theory treats the wake geometry as rigid without interaction between induced velocities and wake structure. The wake structure is assumed to be a flat sheet of vorticity composed of trailing elements whose strength depends on the azimuthal and radial distributions of circulation on a rotor blade. The code predicts the three orthogonal components of flow velocity in the field surrounding the rotor. The predictions can be utilized in rotor performance and helicopter real-time flight-path simulation. The predictive capability of the coded version of the theory was correlated with flow velocity data from several sources. In general, the coded version of flat wake theory provides vertical inflow patterns similar to experimental patterns.

14. SUBJECT TERMS	15. NUMBER OF PAGES
Rotor; Inflow; Wake; Helicopter	51
	16. PRICE CODE A03

17. SECURITY CLASSIFICATION OF REPORT	18. SECURITY CLASSIFICATION OF THIS PAGE	19. SECURITY CLASSIFICATION OF ABSTRACT	20. LIMITATION OF ABSTRACT
Unclassified	Unclassified		

NSN 7540-01-280-5500

Standard Form 298(Rev. 2-89)
Prescribed by ANSI Std. Z39-18
298-102

NASA-Langley, 1992